博士論文

Studies on longevity mechanisms mediated by *S*-adenosyl-L-methionine metabolism in budding yeast

出芽酵母の *S*-アデノシルメチオニン代謝が関与する寿命延長機構に関する研究

小川　貴史

広島大学大学院先端物質科学研究科

2018 年 3 月

目次

(3) Sake yeast *YHR032W/ERC1* haplotype contributes to high *S*-adenosylmethionine accumulation in sake yeast strains
Muneyoshi Kanai, Tomoko Kawata, Yoshie Yoshida, Yasuko Kita, Takafumi Ogawa, Masaki Mizunuma, Daisuke Watanabe, Hitoshi Shimoi, Akihiro Mizuno, Osamu Yamada, Tsutomu Fujii, and Haruyuki Iefuji
Journal of Bioscience and Bioengineering, **123** (1), 8–14 (2017).

(4) メチオニン代謝が鍵となる酵母の長寿の仕組み
小川貴史、水沼正樹
化学と生物、55 巻、8 号、526-528 頁、2017 年

主論文

CONTENTS

INTRODUCTION

Aging is characterized by deterioration in the maintenance of biological functions, leading to an increased risk for major human pathologies, including cancer, diabetes, cardiovascular disorders, and neurodegenerative diseases (Lopez, *et al.*, 2013). With the goal of maintaining human health, the mechanisms of lifespan regulation have been analyzed by using diverse model organisms including yeasts, worms, flies, mice, and monkeys. These analyses have revealed that lifespan is regulated by conserved mechanisms (Kenyon, 2010). Dietary restriction (DR) is defined as a reduction of a particular or total nutrient intake that does not cause malnutrition (Fontana, *et al.*, 2010). DR improves health and increases longevity (Mair, and Dillin, 2008; Fontana, *et al.*, 2010; Kaeberlein, 2010). In particular, calorie restriction (CR) and methionine restriction (MR) extend the lifespan in model organisms (Orentreich, *et al.*, 1993; Miller, *et al.*, 2005; Wu, *et al.*, 2013).

During the last three decades, several nutrition-sensing pathways have been demonstrated to regulate the response to DR (Mair, and Dillin, 2008; Wei *et al.*, 2008). One is the target of rapamycin (TOR) pathway. TOR complex 1 (TORC1) is a highly conserved protein kinase that regulates protein synthesis and growth in response to nutrient intake. Reduction of amino acid intake such as MR is sufficient to extend lifespan in model organisms. Similarly, genetically reduced TOR signaling can extend the lifespan (Mair, and Dillin, 2008). Inhibition of the TORC1-mediated extended lifespan involves the reduction of translation, increased transcription of stress-resistance genes, and promotion of autophagy (Sutter, *et al.*, 2013). Another regulator of DR is AMP-activated protein kinase (AMPK), a highly conserved serine/threonine kinase that monitors the levels of intracellular energy (Hedbacker, and Carlson, 2008). AMPK measures the energy status of cells and functions as a nutrient-sensing switch. Therefore, AMPK has been suggested as having a key role in DR (Mair, and Dillin, 2008). Under a condition of low-energy such as DR, AMPK is activated and promotes catabolism by inhibiting TORC1 in multiple organisms.

Recent studies reported that metabolites such as N-acylethanolamine, α-ketoglutarate, and hydrogen sulfide regulate the activation of the energy-sensing pathways (Lucanic, *et al.*, 2011; Chin, *et al.*, 2014; Hine, *et al.*, 2015). However, while several metabolites have been shown to contribute to the beneficial effects of DR, the molecular mechanism underlying the key metabolites responsible for DR regimens remain unclear.

S-adenosyl-L-methionine (SAM) and *S*-adenosyl-L-homocysteine (SAH) are key intermediates of methionine (Met) metabolism. SAM acts as a methyl group donor of the methylation reaction for nucleic acids, phospholipids, proteins, and other small molecules (Thomas, and Surdin-Kerjan, 1997). SAM-dependent transmethylation is central to the regulation of numerous biological processes, including metabolism, signal transduction, gene expression (Thomas, and Surdin-Kerjan, 1997), and lifespan (Obata, and Miura, 2015; Schosserer *et al.*, 2015). Moreover, after methylation SAM is converted to some metabolites via SAH such as cysteine, glutathione, and polyamine. These metabolites are related to the regulation of lifespan by conferring stress-resistance (Ingenbleek, and Kimura, 2013) and inducing autophagy (Eisenberg. *et al.*, 2009). These studies suggested that SAM has a variety of physiological roles and that intracellular SAM levels affect the progress of aging. However, whether SAM metabolism regulates lifespan is unclear.

The yeast *Saccharomyces cerevisiae* has been used to study aging using two main approaches (Fabrizio, and Longo, 2003; Kaeberlein, 2010). One is replicative lifespan (RLS), which is measured by counting the total number of daughter cells generated from a mother cell. The other is chronological lifespan (CLS), which measures how long yeast cells can survive in a non-dividing state. These two distinct methods are regulated by overlapping but distinct mechanisms (Fabrizio, and Longo, 2003). RLS has been proposed as a model for the aging of mitotically active cells and CLS has been proposed as a model for the aging of post-mitotic cells (Fabrizio, and Longo, 2003; Kaeberlein, 2010).

In this study, a mutant of *S. cerevisiae* featuring an extended CLS with an accumulation of SAM and SAH was isolated. In order to clarify whether SAM and SAH regulated yeast lifespan, the longevity mechanism of this mutant was analyzed. The stimulation of SAM synthesis led to beneficial metabolic effects resulting from the consumption of Met and ATP, which mimicked CR. The stimulated intracellular SAM synthesis extended the lifespan of the yeast cells via activation of AMPK.

CHAPTER I

Isolation and characterization of a longevity mutant which accumulates *S*-adenosyl-L-methionine in budding yeast

1. 1 ABSTRACT

SAM is used for the methylation of diverse molecules in Met metabolism. Several methyltransferases regulated the lifespan of host organisms. However, how SAM metabolism regulated lifespan was not fully understood. To obtain a new lifespan regulator involved in Met metabolism, a mutant of the *SAH1* gene encoding SAH hydrolase was identified. The mutant isolated was designated as *SSG1-1*, for the spontaneous suppression of the growth-delay in *sah1-1*. Interestingly, *SSG1-1* mutant accumulated SAM and SAH, and had an extended chronological lifespan. The longevity mechanism was examined in *SSG1-1* mutant. Stimulating SAM synthesis extended the lifespan in the budding yeast *Saccharomyces cerevisiae* and SAH contributed to longevity with a higher accumulation of SAM.

1. 2 INTRODUCTION

In Met metabolism, SAM is synthesized from Met and ATP, and is used in the methylation reaction of a variety of biological molecules including proteins, phospholipids, and nucleic acids. SAM is converted to SAH after the methylation reaction (Thomas, and Surdin-Kerjan, 1997). Because SAH acts as a competitive inhibitor of the methylation reaction, SAH is immediately degraded by SAH hydrolase (Fig. 1A) (Christopher, *et al.*, 2002).

Recent studies have documented that SAM-dependent transmethylation modulates the lifespan in yeasts, worms, and flies (Greer *et al.*, 2010; Obata, and Miura, 2015; Schosserer *et al.*, 2015). In *Caenorhabditis elegans*, inhibition of the methylation complex of histone H3K4 extended the lifespan, which is associated with formation of germline cells (Greer *et al.*, 2010). Inhibition of methylation of ribosomal RNA can extend lifespan in a manner that is mediated by reduced translation and increased resistance to various stresses in yeasts, worms, and flies (Schosserer *et al*., 2015). Enhanced levels of methylation of glycine-*N*-methyltransferase were able to extend the lifespan of flies by reducing the activity of the insulin signaling pathway (Obata, and Miura, 2015). However, detailed mechanisms of SAM- and SAH-mediated regulation of lifespan were unclear.

The *sah1-1* gene mutant of SAH hydrolase in *S. cerevisiae* was obtained from analysis of the physiological function of calcium ion (Ca^{2+})-signaling. Screening of suppressor mutants of Ca^{2+}-sensitivity from *zds1*Δ cells identified mutant strains that

were classified into 14 genetic complementation groups (*scz1* to *scz14*) (Mizunuma *et al*., 2001; Mizunuma *et al.*, 2004). One of the identified mutants, *scz14*, was identified as a mutant allele of *SIR3*, which is a member of silent information regulator (Sir) complex. The Sir complex participates in chromatin silencing in mating-type loci, telomeres, and ribosomal DNA (Longo, and Kennedy, 2006). NAD-dependent histone deacetylase in Sir complex, Sir2, was required for the extension of RLS in CR (Lin *et al.*, 2000), and the deletion of the *SIR2*, *SIR3*, or *SIR4,* a members of the Sir complex, resulted in a shortened lifespan (Kaeberlein, *et al.*, 1999). These observations suggested that the Sir complex promoted longevity in wild-type (WT) cells. Therefore, our laboratory investigated the relationship between Ca^{2+}-signaling and lifespan in yeast (Tsubakiyama *et al.,* 2011). They found that Δ*zds1* cells had a shortened RLS and constitutively activated calcineurin, Ca^{2+} / Calmodulin-dependent protein phosphatase with high levels of intracellular Ca^{2+}. These results supported the view that *scz* allele was also related to the regulation of lifespan. Indeed, *scz7*, referred to *sah1-1*, accumulated high levels of SAH and SAM, and had a shortened CLS.

In this study, to identify a novel regulator of lifespan involved in Met metabolism, screening was carried out for the suppression of growth-delay of the *sah1-1* cells at elevated temperatures. A suppressor mutant, *SSG1-1,* was identified. *SSG1-1* cells displayed extended CLS with avid accumulation of SAM and SAH. The regulatory mechanism of lifespan was assessed in *SSG1-1* mutant. The results demonstrate that *SSG1-1* increases CLS by stimulating SAM synthesis and that the administration of SAH extends CLS in WT cells by promoting the synthesis of SAM.

1. 3 MATERIAL AND METHODS

1. 3. 1 Yeast strains and media

Yeast strains used in this study were listed in Table 1. All yeast strains were derivatives of W303. Gene disruption was performed by a standard PCR-based method (Longtine *et al.*, 1998). Rich medium (YPD) consisted of 1% yeast extract, 2% polypeptone, 2% glucose, 0.04% adenine hemisulfate and 0.02% uracil. Synthetic complete media SD, SG contain 0.17% Yeast Nitrogen Base without Amino Acid (DIFCO), 0.5% ammonium sulfate, amino acid (contains adenine hemisulfate 20 mg/l, uracil 20 mg/l, tryptophan 20 mg/l, histidine 20 mg/l, arginine 20mg/l, methionine 20mg/l, tyrosine 30mg/l, leucine 30 mg/l, isoleucine 30 mg/l, lysine 30 mg/l, valine 150 mg/l, and

phenylalanine 60mg/l, finaly), 2% of glucose or galactose respectively.

1. 3. 2 Cloning of the mutant *SSG1-1* gene

To identify the *SSG1-1* mutated gene, Tsubakiyama constructed a genomic library in a single-copy plasmid pRS316 by using chromosomal DNA from the *SSG1-1* mutant, because *SSG1-1* was a dominant mutant. The centromeric genomic library was introduced into the *sah1-1* strain, and one plasmid that suppressed the slow-growth phenotype of the *sah1-1* mutant was obtained. The genomic DNA insert in the cloned plasmid *pRT1* (pRS316 based plasmid) (Fig. 1F) was subjected further to restriction mapping and complementation analysis. Partial DNA sequencing of the complementing region revealed that it contained the *YHR032W* gene.

1. 3. 3 Plasmids

pRT1-ΔXbaI, pRT1 A in plasmid, and *YEp24-SSG1-1*/*YEp24-YHR032W* (used in Fig. 1G) were constructed by the following methods. For *pRT1*-ΔXbaI, the *pRT1* plasmid (Fig. 1F) was digested with XbaI, and then self-circularization of linear DNA was performed with DNA Ligation Kit v2.1 (Takara Bio). For *pRT1* A in plasmid, the *pRT1* A in plasmid containing the WT DNA sequence of *YHR032W* was constructed by using a QuikChange XL Site-Directed Mutagenesis Kit (STRATAGENE) and the *pRT1*-ΔXbaI plasmid as a PCR template. The mutagenic primers were 5′-GGTCAAGGGAGACAAAAAAATAGGTGGGTACATC-3′ and 5′-GATGTACC-CACCTATTTTTTTGTCTCCCTTGACC-3′. The mutations were confirmed by DNA sequencing. *YEp24-SSG1-1* and *YEp24-YHR032W*, both the *pRT1*-ΔXbaI plasmid (for *YEp24-SSG1-1*) and the *pRT1* A in plasmid (for *YEp24-YHR032W*) were digested with XbaI-SalI, and cloned into the NheI-SalI–digested YEp24 vector.

1. 3. 4 CLS assay

CLS analysis was performed in liquid SD or SG media that adjusted to pH 6.0, as previously described (Fabrizio *et al.*, 2003). Briefly, SD or SG cultures grown overnight were diluted (2×10^6 cells/mL) in fresh SD or SG media and incubated at 28 °C with shaking at 180 rpm. Viability was measured by plating cells onto YPD plates and monitoring CFUs starting from day 3, which was considered to be the initial survival (100%). All data were represented as the average of three independent experiments conducted at the same time. At least two sets of CLS experiments were performed with

similar outcomes.

1. 3. 5 Isolation of the *SSG1-1* mutants

The *sah1-1* mutants were grown to mid-log phase in liquid YPD medium at 25 °C. The cells were plated onto YPD solid medium at a cell density of 1×10^6 cells per plate and then incubated at 36 °C (high temperature) for 3 days. Approximately 2,500 colonies that grew at this high temperature were picked up. Colonies of suppressor mutants with increased tolerance to the high temperature were spotted onto YPD plates, and the plates were incubated at 37 °C for 2 days. In total, 116 mutants that could grow at 37 °C were obtained. Among these mutants, 15 intragenic suppressors in the *sah1-1* gene were obtained. The remaining 101 suppressor mutants had a dominant mutation, which was classified into one complementation group designated as *SSG1*.

1. 3. 6 Determination of SAM and SAH

Extraction of SAM and SAH was carried out as previously described (Mizunuma *et al.*, 2004). Cells were grown to log phase (2×10^6 cells/mL) in liquid YPD, SD or SG medium at 25 °C. The cells were harvested (total OD_{660} of 15), washed twice with 20 mL of cold water, and then extracted with 1 mL of 10% perchloric acid for 1 h at room temperature. The supernatant was diluted with MilliQ-grade water, and the samples were filtered for capillary electrophoresis. Analysis of SAM and SAH was performed by capillary electrophoresis by using an Agilent Capillary Ion Analyzer G1602A (Agilent) with an Agilent HPCE standard capillary (72-cm total length and 75-μm i.d.). The SAM and SAH contents were expressed as nanomole per milligram dry weight of cells.

1. 3. 7 Stress-resistance assay

Oxidative stress-resistance assays were measured by spot assays. Cells suspended in water (5×10^7 cells/mL) were spotted onto SD or SG plates containing various concentrations of hydrogen peroxide. The cells were then grown at 25 °C for 3 or 4 days before visualization. For heat-shock stress-resistance assays, cells were diluted to 5×10^7 cells/mL and spotted onto YPD plates. The plates were then incubated at 55 °C (heat-shocked) or 25 °C (control) for various times. After the heat-shock, the plates were transferred to 25 °C and incubated for 3 days. For ethionine stress-resistance assays, cells were diluted to 5×10^7 cells/mL and spotted onto SD-Ura-Met or SG-Met

plates containing various concentrations of ethionine. The cells were then grown at 25 °C for 3 or 4 days before visualization.

1. 3. 8 Quantitative real-time PCR analysis

Cells were grown to log phase (2×10^6 cells/mL) in liquid SG medium at 25 °C. Total RNA was isolated from cells using RNeasy Mini Kit (QIAGEN) and quantitative real-time PCR (qRT-PCR) was performed with One Step SYBR Prime Script RT-PCR Kit Ⅱ (Takara) using Light Cycler (Roche). PCR primers for *ACT1* as control were 5'-TTGGATTCCGGTGATGGTGTTACT-3' and 5'-TGAAGAAGATTG-AGCAGCGGTTTG-3'. PCR primers for *SAM1* were 5'-AGGATTTGGAAGACA-TCGGTGC-3' and 5'-CGCTAAAGAGCCATCTCTTCTC-3' and *SAM2* were 5'-CCA-AGGTTGCCTGTGAAACAGC-3' and 5'-GTCGAAACCCTTGGCAGAATCG-3'.

1. 3. 9 Statistical analysis

All experiments were repeated at least twice with similar results each time. Data represent biological replicates. Appropriate statistical tests were used for every figure. GraphPad Prism 6 (GraphPad Software) was used for comparison of CLS, and *P* values were derived from a two-way ANOVA with time and strain used as independent factors and showed in Table 2. The SAM/SAH and the qRT-PCR data were analyzed by appropriate statistical tests (GraphPad Prism 6) as indicated in the figure legends. ImageJ was used to quantify signals for Western blotting results, and GraphPad Prism 6 was used for statistical analysis. *P* values were derived from the two-tailed *t* test, with parametric unequal variance.

1. 4 RESULTS

1. 4. 1 Identification of *SSG1-1* mutants that extended lifespan

The *S. cerevisiae SAH1* was an essential gene for cell growth. Previously Mizunuma *et al.* (2004) found that mutation of *sah1-1* slowed growth at all temperatures examined (25-37 °C) and led to the accumulation of SAH and SAM (Fig. 1B and 1C). Because the homeostasis of cellular metabolism was closely linked to lifespan (Barzilai *et al.*, 2012), Tsubakiyama measured the CLS. As shown in Fig. 1D, the *sah1-1* mutant had a shortened CLS. To obtain a new regulator of the lifespan, Tsubakiyama screened for suppression of the *sah1-1* growth defect at elevated

temperatures (36-37 °C). In this screening, 15 intragenic suppressors in the *sah1-1* gene were obtained. The remaining 101 suppressor mutants had dominant mutations that could be classified into one complementation group, designated *SSG1,* the spontaneous suppression of growth-delay in *sah1-1* mutant (Fig. 1B). One of these mutants, designated *SSG1-1*, was chosen for further study. Cloning and sequencing of the gene that suppressed the slow-growth of the *sah1-1* strain suggested that the *SSG1-1* mutation was an allele of the *YHR032W* gene (Fig. 1E). *YHR032W* had high sequence similarity with the multidrug and toxin extrusion (MATE) family of transporters, and overexpression of the *YHR032W* (designated as *ERC1*) in the *S. cerevisiae* DKD-5D-H strain background, which was a hybrid strain between sake and laboratory yeast, conferred ethionine stress-resistance and SAM accumulation. However, the detail of its function was unknown (Shiomi *et al.*, 1991; Lee, *et al.*, 2010).

Although *SSG1-1* mutants showed resistance to ethionine (Fig. 1G), overexpression of the *YHR032W* (*W303YHR032W*) in W303-1A failed to increase ethionine stress-resistance (Fig. 1G). Moreover, Tsubakiyama showed neither deletion (Tsubakiyama unpublished) nor overexpression of *W303YHR032W* (Fig. 1F) could suppress the slow growth of the *sah1-1* mutant. A comparison of the *SSG1-1* and *W303YHR032W* sequences revealed the presence of a single-base deletion at any one of the seven adenine nucleotide (A) repeats at a position between +1628 and +1634 of the coding region (Fig. 1E). This frameshift mutation was predicted to yield a protein with its C-terminal sequences altered from position 545, resulting in a protein that was 36 amino acids longer relative to Yhr032w. Because the insertion of an A at the same position failed to suppress the slow growth of the *sah1-1* strain (Tsubakiyama unpublished), the A-deletion mutation was suggested to be responsible for the observed phenotypes. Interestingly, it was found that *SSG1-1* had the identical sequences with the *ERC1* gene (Fig. 1E). The nature of the *SSG1-1* may explain the gain-of-function in these phenotypes over the *W303YHR032W* allele. For this reason, I used the *SSG1-1* mutant allele in most of the subsequent experiments.

The growth defect of *sah1-1* was suppressed by exogenous SAM but was not suppressed by SAH (*Mizunuma et al.*, 2004), and overexpression of the *ERC1* resulted in the accumulation of SAM (Shiomi *et al.*, 1991; Lee *et al.*, 2010). Therefore, the ability of the *SSG1-1* mutation to suppress growth-delay of *sah1-1* strain led us to hypothesize that SAM levels might be increased in the *sah1-1 SSG1-1* cells. To test this possibility, I measured SAM levels in cell extracts by performing capillary liquid

electrophoresis analysis. As anticipated, the *sah1-1 SSG1-1* and *SSG1-1* mutants contained higher levels of SAM than *sah1-1* and WT, respectively (Fig. 1C). I found that the SAH levels were also increased in the presence of an *SSG1-1* mutation (Fig. 1C). To investigate whether *SSG1-1* mutation suppressed the short CLS of *sah1-1* cells, I measured the CLS of *sah1-1 SSG1-1* cells and *SSG1-1* cells (Fig. 1D). Indeed, not only *sah1-1 SSG1-1* cells but also *SSG1-1* single mutants were shown to have a longer CLS. It suggested that the Ssg1 protein might play a role in longevity. Because long-lived mutants were occasionally more resistant to oxidative and thermal stress (Lee *et al.*, 2011), I examined the stress-resistance of the *SSG1-1* mutant. As a result, *SSG1-1* mutant showed increased stress-resistance (Fig. 1H). Therefore, I speculated that *SSG1-1* and SAM might be linked to longevity.

1. 4. 2 Stimulating SAM synthesis extended CLS

The SAM synthetase genes (*SAM1* and *SAM2*) of *S. cerevisiae* catalyzed the biosynthesis of SAM (Fig. 1A) (Thomas *et al.*, 1997). Because SAM levels were elevated in *SSG1-1* cells, I determined if CLS extension by *SSG1-1* was mediated by SAM synthesis in the strains deleted for the *SAM1* and *SAM2*. As the growth of *sam1*Δ *sam2*Δ cells was synthetic lethal (Thomas *et al.*, 1997), I constructed *SSG1-1 sam1*Δ and *SSG1-1 sam2*Δ double-mutant strains (Fig. 2A). The SAM levels were lower in both the *SSG1-1 sam1*Δ and *SSG1-1 sam2*Δ compared with the level in the *SSG1-1* cells (Fig. 2B). Indeed, the extended CLS of *SSG1-1* was eliminated by the deletion of either *SAM1* or *SAM2* (Fig. 2C). I next tested whether indeed SAM synthesis extended yeast CLS. I performed aging experiments using WT cells carrying an extra copy of the *SAM1* and *SAM2* genes from the GAL1 promoter integrated into its genome (Fig. 2D). Strikingly, overexpressing *SAM1* and *SAM2* in WT cells significantly extended their CLS (Fig. 2E), concomitant with a high accumulation of SAM (Fig. 2F). In addition, *GAL1-SAM1/2* cells showed resistance to oxidative stress (Fig. 2G).

Although *GAL1-SAM2* cells extended CLS, *GAL1-SAM1* strain did not (Fig. 2E). I examined if CLS extension of *GAL1-SAM2* cells was eliminated by the deletion of *SAM1*. *GAL1-SAM2* Δ*sam1* double-mutant strain was decreased the CLS compared with that of *GAL1-SAM2* strain (Fig. 2H). It was suggested that both *SAM1* and *SAM2* were required for CLS extension by stimulating SAM synthesis.

1. 4. 3 Administration of SAH extended CLS via stimulating SAM synthesis

The supplementing the medium with SAM was unable to extend the CLS of the WT cells (Fig. 3A and 3B). In contrast, extracellular SAH contributed to an extended the CLS with a high accumulation of SAM than of SAH (Fig. 3A and 3C). It should be noted that I could not detect the SAM or SAH levels in the culture medium in this experiment. Although the supplementing the medium with SAM was unable to extend the CLS of the Δ*sam1* cells (Fig. 3D and 3E), externally added SAH also had no effect on the CLS of *sam1*Δ in which the increase in their SAM level was not more than that of SAH (Fig. 3D and 3F). Taken together, these data showed that CLS extension by *SSG1-1* was dependent on SAM synthesis and suggested that stimulating SAM synthesis *per se* could promote longevity.

1. 4. 4 Effects of stimulating SAM synthesis on *sah1-1* mutant or resistance to ethionine

The *sah1-1* mutant displayed accumulation of SAM (Fig. 1C) (Mizunuma *et al.*, 2004). However, whether this accumulation occurred due to by *SAM1* or *SAM2* was unclear. Presently, the effect of the deletion of *SAM1* or *SAM2* in the *sah1-1* mutant on the accumulation of SAM was investigated. The *sah1-1 sam1*Δ and *sah1-1 sam2*Δ cells displayed decreased accumulation of SAM compared to *sah1-1* cells (Fig. 4A). This suggested that *sah1-1* cells accumulated SAM by *SAM1* and *SAM2*. To clarify the necessity of *SAM1* or *SAM2* in the CLS of *sah1-1* mutant, CLS was analyzed in the *sah1-1 sam1*Δ and *sah1-1 sam2*Δ mutants. Unexpectedly, these mutants had the CLS as long as that of *sah1-1* cells (Fig. 4B), suggesting that synthesis of SAM did not affect the CLS of the *sah1-1* mutant.

The *sah1-1 SSG1-1* double mutant restored the growth delay of *sah1-1* cells and the accumulation of the SAM was evident compared with *sah1-1* cells (Fig. 1B and 1C). Whether the overexpression of *SAM1* and *SAM2* in *sah1-1* cells could suppress the growth-delay of *sah1-1* cells was investigated next. For this, *sah1-1 GAL1-SAM1/2* cells were constructed. The cells did not suppress the growth-delay of *sah1-1* cells (Fig. 4C), suggesting that *SSG1-1* had an unknown function for the suppression of the growth-delay of *sah1-1* cells. Moreover, it was reported that deletion of adenosine kinase, *ADO1*, led to the accumulation of SAM in yeast (Kanai *et al.,* 2013). However, the *sah1-1 ado1*Δ double-mutant did not display restoration of the growth-delay of *sah1-1* cells (Fig. 4D). The observation suggested that suppression of the growth-delay

of *sah1-1* cells was not able to explain the levels of accumulation of SAM.

Because *SSG1-1* mutants showed resistance to ethionine (Fig. 1G), it was appropriate to investigate whether *GAL1-SAM1/2* also conferred resistance to ethionine. *GAL1-SAM1/2* did not show this resistance (Fig. 4E), suggesting that stimulating SAM synthesis did not affect the resistance to ethionine. Therefore, Ssg1 has an unknown mechanism of resistance to ethionine.

1. 5 DISCUSSION

The experiments in this chapter demonstrated that *SSG1-1* strain possessing a mutation in *YHR032W* gene extended CLS by stimulating SAM synthesis (Fig. 1C, 1D, and 1E). Interestingly, industrial yeast genes like *sakeYHR032W* in the sake yeast Kyokai no. 7 strain and *ERC1* in the sake-laboratory strain hybrid DKD-5D-H had the same sequence of *SSG1-1.* On the other hand, genes from laboratory yeasts *W303*, *S288C*, and FL100, but not from Σ1278b, did not possess an adenine nucleotide deletion (Fig. 1E) (Akao, *et al.*, 2011). Moreover, sake yeast accumulated SAM (Shimizu, *et al.*, 1984). These results suggested that *ERC1*/*sakeYHR032W* was the gene responsible for an accumulation SAM in sake yeast. Indeed, a recent analysis of the quantitative trait loci (QTL) identified genes associated with the accumulation of SAM. The genes included *ERC1* in the sake yeast strain Kyokai no. 7 (Kanai, *et al.*, 2017). Stimulating SAM synthesis conferred stress-resistance, suggesting that it might be advantageous to reserve Met and ATP in the form of SAM to confer stress resistance and longevity to overcome periods of excess glucose/ATP that occur during fermentation. In their natural environment yeasts were faced with variable carbon supplies and, therefore, accumulated SAM as a stable energy and nutrient source. In contrast, the laboratory yeast *YHR032W* locus might have lost this behavior during evolution because of the proper/controlled amount of nutrients that promoted cell growth. In this regard, it was worth noting that *SSG1-1* mutation could be readily generated by a single-base deletion at any one of the seven repeats of the adenine nucleotide and, conversely, that the reverse mutations would be facilitated by the insertion of a single adenine nucleotide to the repeated sequences in response to environment changes.

Christopher *et al.* (2002) proposed that the SAM:SAH ratio was important and that there was no growth inhibitory effect if the ratio exceeded a threshold value. Consistent with their observations, the inhibitory effect of SAH was presently abrogated

in the simultaneous presence of SAM (Mizunuma, *et al.*, 2004). However, it seemed difficult to explain the negative or positive physiological effects because of cellular accumulation of SAM and SAH simply in terms of the SAM:SAH ratio. The accumulation of SAH *per se* appeared to inhibit cell growth and increased the sensitivity to stress in the *sah1-1* strain (Mizunuma, *et al.*, 2004). In contrast, although the SAM:SAH ratio in the *SSG1-1* strain was apparently similar to that of the *sah1-1* strain, the cell growth was at the level of the WT, with superior stress resistance than the WT.

Why did the *SSG1-1* mutant, but not the *sah1-1* mutant, have an extended CLS, despite the accumulation of SAM and SAH in both strains (Fig. 1C and 1D)? The deletion of *SAM1* or *SAM2* in *SSG1-1* mutant reduced the SAM levels, leading to a loss of the beneficial effect on CLS (Fig. 2B and 2C). The *sah1-1* strain also showed reduced levels of SAM when *SAM1* or *SAM2* was deleted (Fig. 4A), suggesting that *sah1-1* and *SSG1-1* accumulated SAM by the same mechanism. However, the CLS of *sah1-1* cells was unaffected by the deletion of *SAM1* or *SAM2* (Fig. 4B). Therefore, some additional mechanisms appeared to be operative concerning the effects of SAM and SAH on CLS. Elevated levels of SAM were detrimental to yeast if the excess SAM cannot be sequestered in the cell vacuole (Jacquemin-Faure *et al.*, 1994; Chan, and Appling, 2003). Thus, the beneficial effect of *SSG1-1* on lifespan may be explained by the accumulation of SAM and SAH in the yeast vacuole. This possibility warrants further study.

A previous study in our laboratory proposed that the elevation of the cellular SAM level in *sah1-1* cells could be the result of the activation of an unidentified compensatory mechanism to alleviate the inhibitory effect of SAH on cell growth (Mizunuma *et al.*, 2004). The present findings shed additional light on the effect of SAH in yeast. When *SAM1/2* was overexpressed or SAM was administered, the cells did not accumulate SAH (Fig. 2F and Fig. 3B). In contrast, administration of SAH caused the stimulation of SAM synthesis in WT cells (Fig. 3C), as in the *sah1-1* cells. Moreover, externally added SAH, but not SAM, extended the CLS (Fig. 3A). Thus, an unidentified compensatory mechanism to alleviate the inhibitory effect of SAH on cell growth will be important for this lifespan extension.

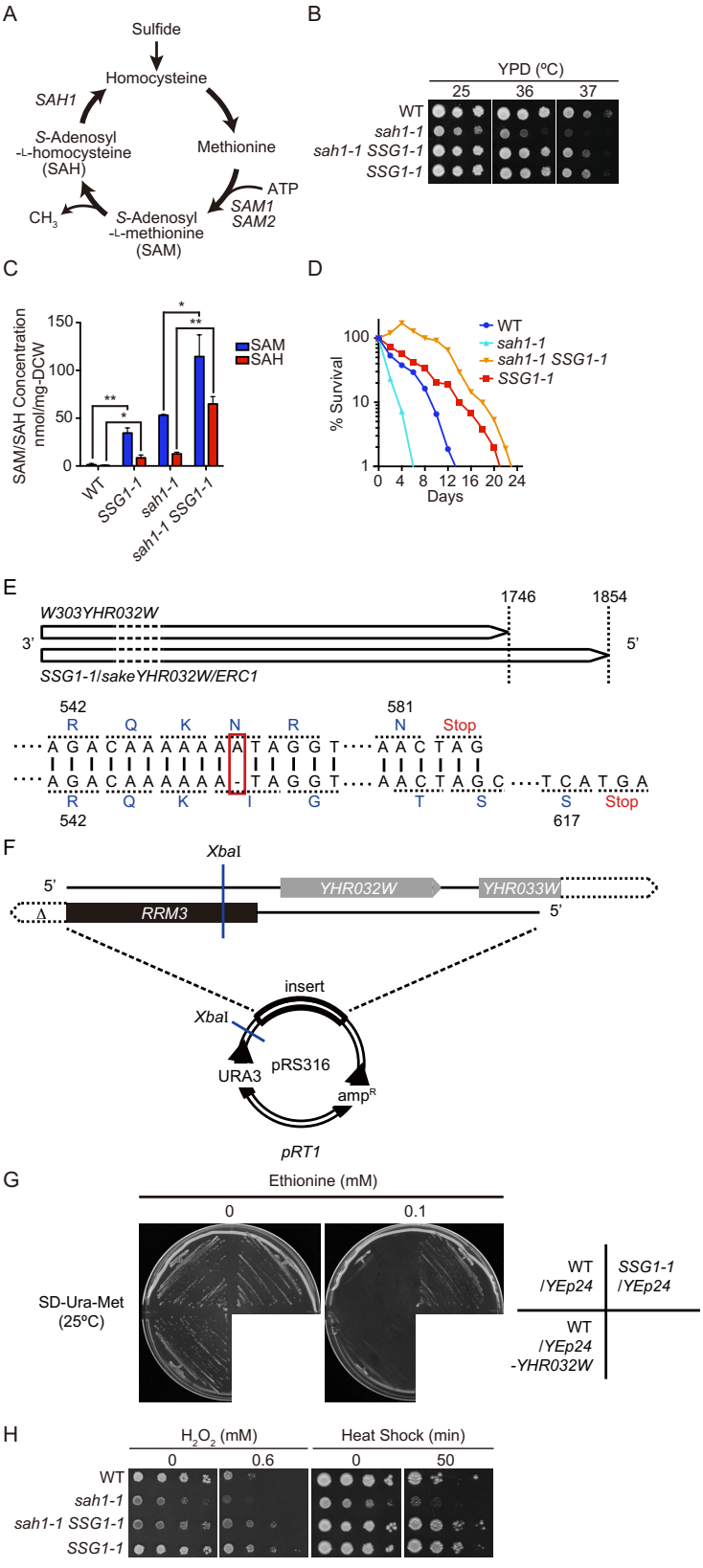
A
Sulfide
Homocysteine
SAH1
S-Adenosyl
-L-homocysteine
(SAH)
Methionine
ATP
SAM1
SAM2
CH3
S-Adenosyl
-L-methionine
(SAM)
B
YPD (ºC)
25
36
37
WT
sah1-1
sah1-1 SSG1-1
SSG1-1
C
SAM/SAH Concentration
nmol/mg-DCW
150
100
50
0
SAM
SAH
WT
SSG1-1
sah1-1
sah1-1 SSG1-1
D
% Survival
100
10
1
0 4 8 12 16 20 24
Days
WT
sah1-1
sah1-1 SSG1-1
SSG1-1
E
W303YHR032W
SSG1-1/sakeYHR032W/ERC1
3'
5'
1746
1854
542
581
R Q K N R
N Stop
A G A C A A A A A A T A G G T
A G A C A A A A A - T A G G T
A A C T A G
A A C T A G C
T C A T G A
R Q K I G
T S
S Stop
542
617
F
XbaI
5'
YHR032W
YHR033W
Δ
RRM3
5'
insert
XbaI
URA3
pRS316
ampR
pRT1
G
Ethionine (mM)
0
0.1
SD-Ura-Met
(25ºC)
WT
/YEp24
SSG1-1
/YEp24
WT
/YEp24
-YHR032W
H
H2O2 (mM)
0
0.6
Heat Shock (min)
0
50
WT
sah1-1
sah1-1 SSG1-1
SSG1-1

Fig. 1 *SSG1-1* suppressed growth-delay of the *sah1-1* strain and extended CLS.[#]
(A) Schematic diagram of methionine metabolism. (B) Growth of various strains on solid YPD medium. Serial dilutions of cells were spotted onto the plates, which were then incubated for 2~3 days at 25 °C, 36 °C, or 37 °C. (C) Intracellular SAM and SAH levels in YPD medium. Mean ± SD (n = 3); **P* < 0.05; ***P* < 0.01 (*t* test, two-tailed, parametric unequal variance). (D) CLS curve. (E) Diagrams of *YHR032* and *SSG1-1* sequences showing the mutation site. (F) Map of the ORFs inserted in plasmid pRT1. (G) Ethionine resistance-test. Cells harboring the indicated plasmids were streaked onto SD-Ura-Met plates with or without 0.1 mM ethionine and grown at 25 °C for 3 days. (H) Hydrogen peroxide stress and heat-shock stress tests. Ten-fold serially diluted cells were spotted onto solid medium containing 0.6 mM hydrogen peroxide (SD plates at 25 °C) or were subjected to heat-shock treatment at 55 °C in YPD plates, which were then transferred to 25 °C and incubated for 3 days. # Fig. 1 was cited and modified from Ogawa *et al.*, 2016.

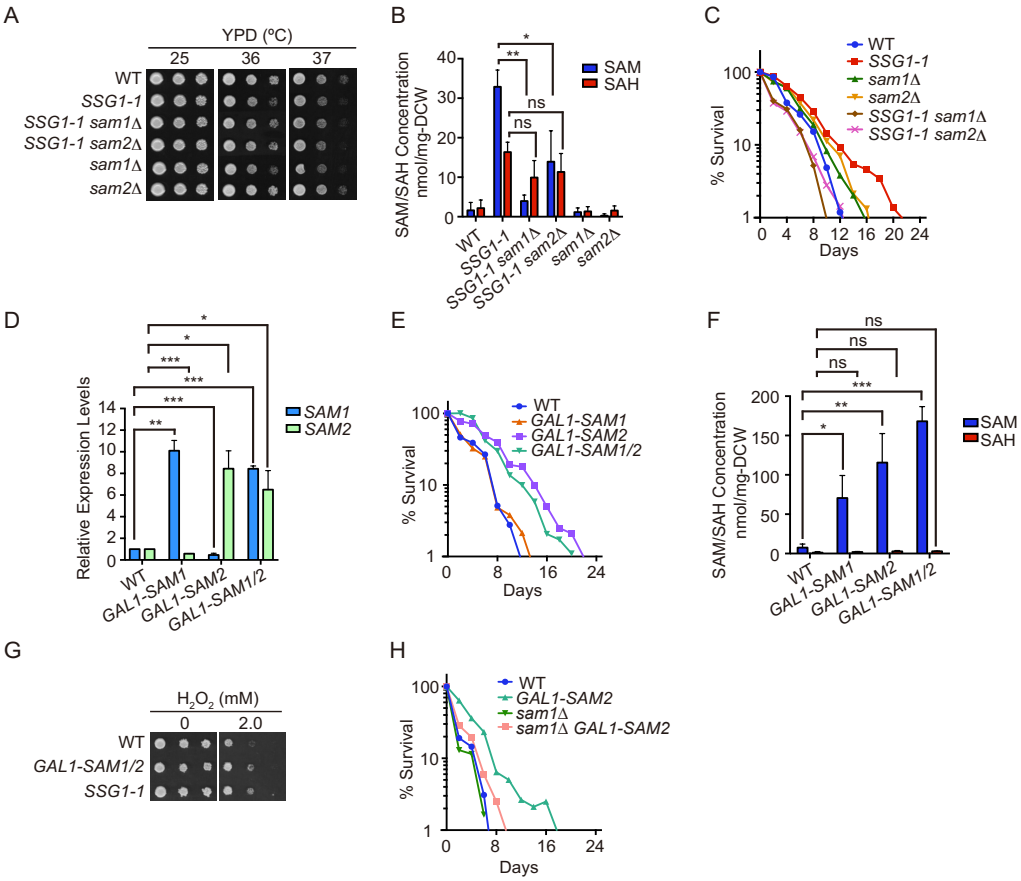

Fig. 2 Stimulating SAM synthesis extended CLS and increased stress-resistance.[#]
(A) Growth of various strains on solid YPD medium. (B) The SAM and SAH contents were measured in SD medium. Mean ± SD (n = 3); ns, not significant; **P* < 0.05; ***P* < 0.01 (*t* test, two-tailed, parametric unequal variance). (C) CLS curve. (D) Relative expression level of *SAM1/2* measured by reverse transcription real-time PCR in SG medium. Mean ± SD (n = 2); **P* < 0.05; ***P* < 0.01; ****P* < 0.001 (*t* test, two-tailed, parametric unequal variance). (E and F) Effect of overexpression of *SAM1* and *SAM2* in WT on CLS (E) and on SAM and SAH levels (F). Cells in SG medium (+ 2% galactose medium, GAL1 promoter turned on) were measured. ns, not significant; ****P* < 0.001 (*t* test, two-tailed, parametric unequal variance). (G) Hydrogen peroxide stress tests. Ten-fold serially diluted cells were spotted onto solid medium containing 2.0 mM hydrogen peroxide (SG plates at 25 °C), which were then transferred to 25 °C and incubated for 4 days. (H) Effect of *SAM1* deletion for *GAL1-SAM2* strain on CLS. # Fig. 2 was cited and modified from Ogawa *et al.*, 2016.

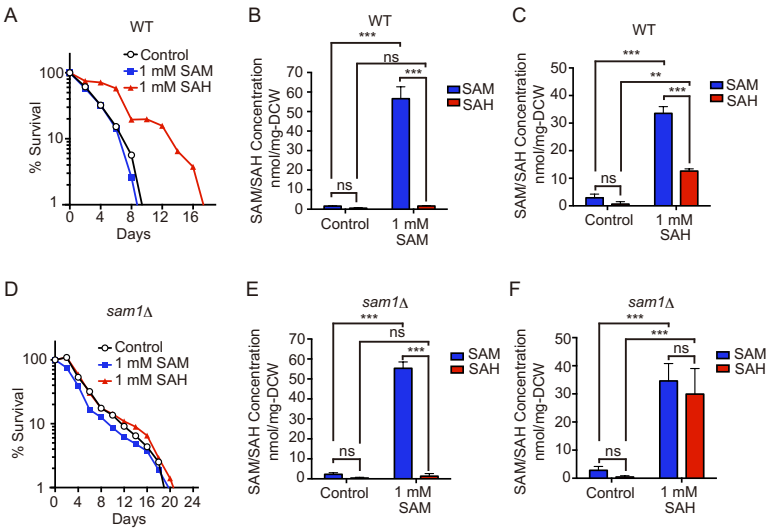

Fig. 3 Administration of SAH extended CLS via stimulating SAM synthesis.[#]
(A–F) Effect of SAM or SAH administration on CLS (A and D) and on SAM and SAH levels (B, C, E and F) of WT or *sam1Δ* cells. Intracellular SAM and SAH levels were quantified. Mean ± SD (n = 3); ns, not significant; $^{**}P < 0.01$; $^{***}P < 0.001$ (two-way ANOVA with Tukey's multiple comparisons test, A and D). # Fig. 3 was cited and modified from Ogawa *et al.*, 2016.

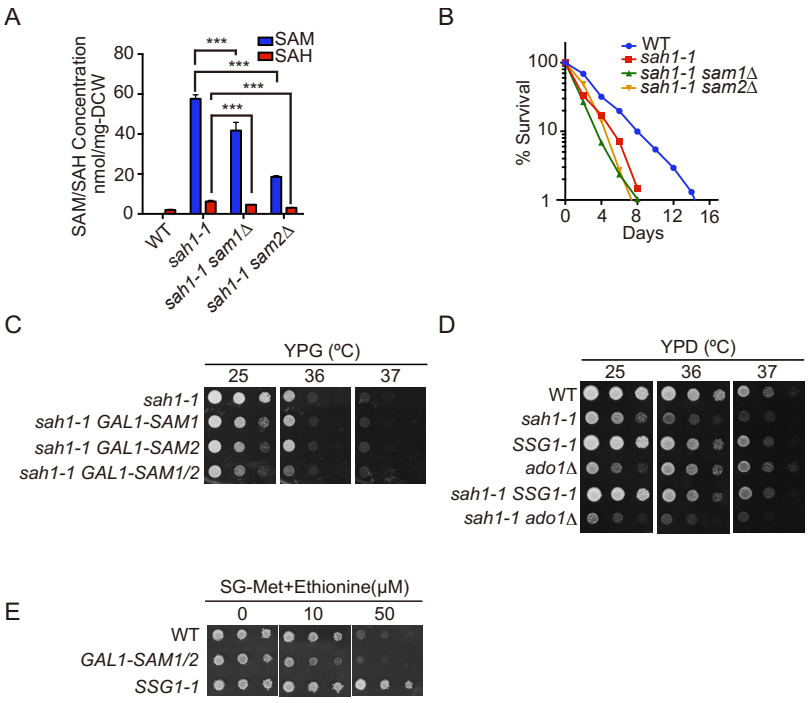

Fig. 4 Effects of stimulating SAM synthesis on *sah1-1* mutant or resistance to ethionine.[#]

(A) The SAM and SAH contents were measured. Mean ± SD (n = 3); ***$P < 0.001$ (*t* test, two-tailed, parametric unequal variance). (B) CLS curves were shown. (C and D) Growth of various strains on solid YPG medium (C) and YPD medium (D). (E) Ethionine stress test. Cells were spotted onto solid medium containing and 10 or 50 μM ethionine (SG-Met plates at 25ºC), which were then transferred to 25 °C and incubated for 3 days. # Fig. 4 was cited and modified from Ogawa *et al.*, 2016.

Table 1 Strains used in Chapter I

Strain	Genotype	Source or Reference
W303-1A	MATa; *trp1, leu2, ade2, ura3, his3, can1-100*	Lab. stock
YMM222	MATa; *sah1-1* [W303-1A]	Mizunuma *et al*., 2004
YRT15	MATa; *SSG1-1* [W303-1A]	this study
YRT3	MATa; *sah1-1 SSG1-1* [W303-1A]	this study
YTO29	MATa; *sam1Δ::kanMX4* [W303-1A]	this study
YTO35	MATa; *sam2Δ::kanMX4* [W303-1A]	this study
YTO33	MATa; *SSG1-1 sam1Δ::kanMX4* [W303-1A]	this study
YTO39	MATa; *SSG1-1 sam2Δ::kanMX4* [W303-1A]	this study
YTO66	MATa; *sah1-1 sam1Δ::kanMX4* [W303-1A]	this study
YTO67	MATa; *sah1-1 sam2Δ::kanMX4* [W303-1A]	this study
YTO73	MATa; *GAL1-SAM1* [W303-1A]	this study
YTO75	MAT1; *GAL1-SAM2* [W303-1A]	this study
YTO78	MATa; *GAL1-SAM1 GAL1-SAM2* [W303-1A]	this study
YTO87	MATa; *sah1-1 GAL1-SAM1* [W303-1A]	this study
YTO89	MATa; *sah1-1 GAL1-SAM2* [W303-1A]	this study
YTO91	MATa; *sah1-1 GAL1-SAM1 GAL-SAM2* [W303-1A]	this study
YTO96	MATa; *sam1Δ::kanMX4 GAL1-SAM2* [W303-1A]	this study
W/Δado1	MATa; *ado1Δ::kanMX4* [W303-1A]	this study
YTO10	MATa; *sah1-1 ado1Δ::kanMX4* [W303-1A]	this study

Table 2 *P* values for chronological lifespan analysis

Figure	Strain A	Strain B	*P*-value against B
Fig. 1D	WT	*sah1-1*	< 0.0001
	WT	*sah1-1 SSG1-1*	< 0.0001
	WT	*SSG1-1*	< 0.0001
	sah1-1	*sah1-1 SSG1-1*	< 0.0001
Fig. 2C	WT	*sam1*Δ	0.4655
	WT	*sam2*Δ	0.0612
	WT	*SSG1-1 sam1*Δ	< 0.0001
	WT	*SSG1-1 sam2*Δ	< 0.0001
	SSG1-1	*SSG1-1 sam1*Δ	< 0.0001
	SSG1-1	*SSG1-1 sam2*Δ	< 0.0001
Fig. 2E	WT	*GAL1-SAM1*	0.9812
	WT	*GAL1-SAM2*	0.0021
	WT	*GAL1-SAM1/2*	< 0.0001
Fig. 2H	*GAL1-SAM2*	*GAL1-SAM2 sam1*Δ	0.0043
Fig. 3A	WT (Control)	WT (+ 1mM SAM)	0.8140
	WT (Control)	WT (+ 1mM SAH)	< 0.0001
Fig. 3D	*sam1*Δ (Control)	*sam1*Δ (+ 1mM SAM)	0.0141
	*sam1*Δ (Control)	*sam1*Δ (+ 1mM SAH)	0.8812
Fig. 4B	WT	*sah1-1 sam1*Δ	< 0.0001
	WT	*sah1-1 sam2*Δ	< 0.0001
	sah1-1	*sah1-1 sam1*Δ	0.1231
	sah1-1	*sah1-1 sam2*Δ	0.8611

P values were derived from a two-way ANOVA with time and strain used as independent factors.

CHAPTER II
Analysis of longevity mechanisms involved in the stimulation of *S*-adenosyl-L-methionine synthesis in budding yeast

2. 1 ABSTRACT

Stimulating SAM synthesis prolonged the CLS in *SSG1-1* mutant, which accumulated high levels of SAM and SAH. To clarify the basis for the synthesis of SAM mediated longevity, DNA microarray analyses were conducted with the *SSG1-1* mutant. The mutant displayed up-regulated expression of the genes for Met metabolism and glucose metabolism that was associated with CR. Moreover, the *SSG1-1* mutant consumed both Met and ATP, and displayed an extended CLS epistatic to CR. Stimulating SAM synthesis activated the universal energy-sensing regulator Snf1, which is the ortholog of AMPK, and resulted in the extension of lifespan.

In order to clarify the physiological significance of an accumulation of SAM, the accumulation levels of SAM and SAH were examined in CR conditions. WT cells displayed an extended CLS with an increased SAM and SAH levels at 0.05% glucose concentration. The data uncover the molecular links between Met metabolites and lifespan, suggesting a unique function of SAM as a reservoir of Met and ATP for cell survival.

2. 2 INTRODUCTION

In Chapter I, the *SSG1-1* mutant displaying accumulated SAM and SAH was isolated as the suppressor of the growth delay of the *sah1-1* mutant. *SSG1-1* mutant showed the extension of CLS by stimulating SAM synthesis. Moreover, the administration of SAH also stimulated SAM synthesis and increased CLS in WT cells. However, the mechanisms of longevity related to stimulated SAM synthesis and physiological function to accumulate SAM or SAH remained unknown.

Snf1 is an AMPK in yeast that functions as an intracellular energy sensor. Decreasing the ratio of intracellular ATP/ADP activates Snf1 and promotes the catabolism and induced expression of genes expressed during glucose starvation (Ghillebert *et al*., 2011). Although Snf1 was reportedly activated in CR, whether Met metabolism extended CLS via activation of Snf1 was not clear (Mair, W., and Dillin, A. 2008).

In Chapter II, to clarify the mechanisms of extended CLS by the stimulated synthesis of SAM, the transcriptional profile in the *SSG1-1* mutant was analyzed. The mutant consumed both Met and ATP, and regulated nutrition metabolism, which resulted in the extension of CLS. Stimulating SAM synthesis led to AMPK activation.

In *Schizosaccharomyces pombe,* cells accumulated SAM in CR condition (0.04% glucose concentration) (Plaskal *et al*., 2011), suggesting that SAM synthesis was promoted during severe nutrition depletion. However, the physiological significance of the accumulation of SAM had been unclear. Here, the importance of the accumulation of SAM to lifespan was explored by examining whether SAM accumulated in a severe CR condition (0.05% glucose concentration) and whether it linked to lifespan extension in *S. cerevisiae*.

2. 3 MATERIALS AND METHODS

2. 3. 1 Yeast strains and media

Yeast strains used in this study were listed in Table 3. All yeast strains were derivatives of W303. Gene disruption was performed by a standard PCR-based method (Longtine *et al.*, 1998). Rich medium (YPD) consisted of 1% yeast extract, 2% polypeptone, 2% glucose, 0.04% adenine hemisulfate and 0.02% uracil. Synthetic complete media SD, SG contain 0.17% Yeast Nitrogen Base without Amino Acid (DIFCO), 0.5% ammonium sulfate, amino acid (contains adenine hemisulfate 20 mg/l, uracil 20 mg/l, tryptophan 20 mg/l, histidine 20 mg/l, arginine 20mg/l, Methionine 20mg/l, tyrosine 30mg/l, leucine 30 mg/l, isoleucine 30 mg/l, lysine 30 mg/l, valine 150 mg/l and phenylalanine 60mg/l, finaly), 2% of glucose or galactose respectively.

2. 3. 2 CLS assay

CLS analysis was performed in liquid SD media that adjusted to pH 6.0, as previously described (Fabrizio *et al.*, 2003). Briefly, SD cultures grown overnight were diluted (2×10^6 cells/mL) in fresh SD media and incubated at 28 °C with shaking at 180 rpm. Viability was measured by plating cells onto YPD plates and monitoring CFUs starting from day 3, which was considered to be the initial survival (100%). All data were represented as the average of three independent experiments conducted at the same time. At least two sets of CLS experiments were performed with similar outcomes.

2. 3. 3 Microarray analysis

RNA isolation and microarray profiling analyses were carried out as previously described (Kanai *et al.*, 2013; Shobayashi *et al.*, 2007), using the Gene Chip Yeast Genome 2.0 Array (Affymetrix). Cells were grown to early log phase (2×10^6 cells/mL)

in liquid SD medium at 28 °C. A given gene was considered induced when its expression ratio was higher than 2.0. Microarray data have been deposited at the public repository Gene Expression Omnibus (GEO) under accession number GSE76206.

2. 3. 4 Determination of SAM and SAH

Extraction of SAM and SAH was carried out as previously described (Mizunuma *et al.*, 2004). Cells were grown to log phase (2×10^6 cells/mL) in liquid SD medium at 25 °C. The cells were harvested (total OD_{660} of 15), washed twice with 20 mL of cold water, and then extracted with 1 mL of 10% perchloric acid for 1 h at room temperature. The supernatant was diluted with MilliQ-grade water, and the samples were filtered for capillary electrophoresis. Analysis of SAM and SAH was performed by capillary electrophoresis by using an Agilent Capillary Ion Analyzer G1602A (Agilent) with an Agilent HPCE standard capillary (72-cm total length and 75-μm i.d.). The SAM and SAH contents were expressed as nanomole per milligram dry weight of cells.

2. 3. 5 Determination of Met

Cells were grown to log phase (5×10^6 cells/mL) in liquid SD medium at 25 °C. The cells were harvested by centrifugation to 3×10^8 cells and washed twice with cold MilliQ-grade water. The cell pellet was extracted amino acid with 1.1 mL of 60% methanol by rotation for 15 min at 28 °C. After centrifugation at 21,600 × g for 5 min, the supernatant was store at -80 °C. For the methionine measurement, the amino acid solution was filtered by Ekicrodisc (Pall Corp.) and measured using an amino acid analyzer (JLC-500 amino acid analyzer, JEOL).

2. 3. 6 Determination of ATP

Cells were grown to log phase (5×10^6 cells/mL) in liquid SD medium at 25 °C. The cells were harvested by centrifugation to 2×10^7 cells (860 × g, 5 min). The cell pellet was washed by MilliQ-grade water three times and stored at -80 °C. The cell pellet was resuspended in 100 μL MilliQ-garade water and lysed cells by boiling for 10 min to extract intracellular ATP. The lysed sample was centrifuged at 4 °C and 16,200 × g for 5 min. For the ATP measurement, 200 μL of the solution was mixed with 100 μL of ATP assay buffer (Kikkoman Biochemifa) and measured fluorescence using LUMITESTER C-110 (Kikkoman Biochemifa).

2. 3. 7 Quantitative real-time PCR analysis

Cells were grown to log phase (2×10^6 cells/mL) in liquid SD medium at 25 °C. Total RNA was isolated from cells using RNeasy Mini Kit (QIAGEN) and qRT-PCR was performed with One Step SYBR PrimeScript RT-PCR Kit Ⅱ (Takara) using Light Cycler (Roche). PCR primers for *ACT1* as control were 5'-TTGGATTCCGGTGATGG-TGTTACT-3' and 5'-TGAAGAAGATTGAGCAGCGGTTTG-3'. PCR primers for *COX3* were 5'-AATGCATGGTTATATTGGTAAT-3' and 5'-AGCTTCAGCTACAAT-ATCTCTAA-3'.

2. 3. 8 Detection of Snf1 activation

Protein extraction was carried out as described previously (Orlova *et al.*, 2008). An exponentially grown cell culture (5×10^6 cells/mL) in SD or SG liquid medium was boiled for 5 min and then cooled to room temperature. The cells were harvested by centrifugation, and the pellets were resuspended in 150 μL 1× TE buffer [10 mM Tris·HCl, 1 mM EDTA (pH 7.5)] following the addition of 150 μL of 0.2 M NaOH. After incubation for 5 min at room temperature, the pellets were collected, gently resuspended in SDS/PAGE sample buffer, and boiled for 5 min. The eluted proteins were resolved by SDS/PAGE and detected with Phospho-AMPKα (Thr172) antibody (Cell Signaling). For detection of total Snf1 protein, polyhistidine antibody H1029 (Sigma-Aldrich) was used.

2. 3. 9 Statistical analysis

All experiments were repeated at least twice with similar results each time. Data represent biological replicates. Appropriate statistical tests were used for every figure. GraphPad Prism 6 (GraphPad Software) was used for comparison of CLS, and *P* values were derived from a two-way ANOVA with time and strain used as independent factors and showed in Table 5. The SAM/SAH and the qRT-PCR data were analyzed by appropriate statistical tests (GraphPad Prism 6) as indicated in the figure legends. ImageJ was used to quantify signals for Western blotting results, and GraphPad Prism 6 was used for statistical analysis. *P* values were derived from the two-tailed *t* test, with parametric unequal variance. A *P* value less than 0.05 was defined as statistically significant except for microarray data ($P < 0.1$, unpaired *t* test).

2. 4 RESULTS

2. 4. 1 Stimulating SAM synthesis-mediated longevity was epistatic to CR

To identify longevity mechanisms of the *SSG1-1* mutant in detail, I conducted DNA microarray analysis using *SSG1-1* and WT cells. In this experience, I identified genes whose expression was increased more than twofold in the *SSG1-1* cells. In total, 21 genes were up-regulated which included the genes involved in Met metabolism such as *MHT1* (*S*-methylmethionine methyltransferase) and *MET14* (adenylylsulfate kinase) (Table 4). It was consistent with the high accumulation of SAM in the *SSG1-1* cells (Fig. 1C). In addition, I also found genes involved in glucose metabolism such as *HXT4* (high-affinity glucose transporter) and *HXK1* (hexokinase), which were associated with CR (0.5% glucose) (Table 4) (Lee and Lee, 2008). These data suggested that *SSG1-1* and CR shared a common pathway to confer longevity.

SAM synthesis required both Met and ATP (Fig. 1A). In *SSG1-1* cells, which can consume Met and ATP during chronological aging, higher amounts of SAM accumulated (Fig. 1C). All organisms produce ATP by glycolysis through the degradation of glucose. MR or CR was reported to extend the lifespan in many eukaryotes (Mayer, and dillin, 2008, Miller *et al.*, 2005). Thus, I assumed that consumption of Met and glucose for SAM synthesis was required for extended CLS in *SSG1-1* and the CLS of *SSG1-1* would diminished by limiting either the Met or glucose concentration in the medium. Indeed, when the medium was shifted from original medium (contains 20 mg/l methionine) to the Met-depleted medium (0 mg/l methionine), the lifespan of *SSG1-1* cells was suppressed as long as WT cells (Fig. 5A). Besides, I found that when the glucose concentration was limited to 0.05%, the CLS of *SSG1-1* did not extended (Fig. 5B). On the other hand, I found that treatment with 0.05% glucose slightly but reproducibly increased the maximum CLS of the WT (Fig. 5B). These results support the idea that consumption of Met and ATP in the *SSG1-1* cells contributed to the extended CLS. It should be noted that whereas *SSG1-1* was a methionine-prototrophic strain, the CLS of *SSG1-1* was not extended when Met was depleted from the medium, suggesting that the intake of extracellular Met was required for lifespan extension.

From these analyses, Met and ATP concentrations were expected to decrease in *SSG1-1* cells. As a result, Met concentration in *SSG1-1* cells was lower than that of WT cells (Fig. 5D). On the contrary, intracellular ATP levels were more increased than that of WT cells (Fig. 5E). This result suggested that *SSG1-1* cells kept their ATP levels

higher for synthesis of SAM.

A 0.5% glucose concentration has been used for CR studies in yeast, resulting in an extended CLS (Fabrizio, and Longo, 2003). I next measured that the lifespan of *SSG1-1* cells in CR (0.5% glucose), and found that the CLS of *SSG1-1* strain was equivalent to that of WT strain (Fig. 5C), suggesting that a common pathway under lie regulatory mechanism for longevity between CR and *SSG1-1*-mediated mechanism.

2. 4. 2 Stimulating SAM synthesis led to AMPK activation

Snf1 was the central component of the glucose-repression pathway and was orthologous to the mammalian AMPK (Headbacker, and Carlson, 2008). Thus, I anticipated that Snf1 would be activated in the *SSG1-1* cells. Snf1 activity can be monitored by the phosphorylation of residue Thr210 of Snf1 (Orlova *et al.*, 2008). Compared with that in WT cells, phosphorylation of Thr210 was increased in *SSG1-1* cells (Fig. 6A), supporting the hypothesis that Snf1 was indeed activated. I confirmed that stimulating SAM synthesis modulated the activity of Snf1. I found that overexpression of *SAM1* and *SAM2* did cause an increase in Snf1 phosphorylation (Fig. 6B). Snf1 activity correlates with a high ADP:ATP ratio (Mayer *et al.*, 2011); however, Snf1 was activated in the *SSG1-1* cells even though the ATP level was increased (Fig. 5E). These seemingly paradoxical results led us to examine the effect of *SNF1* deletion on ATP levels in the *SSG1-1* cells. I found that ATP levels were decreased in the *SSG1-1 snf1Δ* mutants (Fig. 5E), suggesting that Snf1 enhanced processes that generated ATP or inhibited others that consumed ATP when cells were stimulated to have higher SAM levels, as in the *SSG1-1* cells. Interestingly, I found that SAM levels were reduced in the *SSG1-1 snf1Δ* mutants (Fig. 6C). Together, these data suggested that Snf1 was activated by stimulating SAM synthesis, which contributed to sustaining SAM levels by amplifying ATP (Fig. 5E). This mechanism of action is the subject of future investigations.

To test the role of *SNF1* in CLS, I measured the CLS of *SSG1-1 snf1Δ* mutants and *SSG1-1 snf1Δ* mutants was decreased CLS compared with that of the *SSG1-1* (Fig. 6D), suggesting that Snf1 might had been required for extending the CLS of *SSG1-1*. However, because the *SNF1* single-deletion mutants showed a shortened CLS (Fig. 6D), it was difficult to conclude that Snf1 mediated the CLS extension in *SSG1-1*. These results suggested that the beneficial effect of stimulating SAM synthesis was exerted, at least in part, through the activation of Snf1 (Fig. 6E).

It was known that when yeast performed CR, they converted their metabolism from anaerobic metabolism to aerobic metabolism in the logarithmic growth phase (Ocampo *et al.*, 2013). Because Snf1 activated catabolism, I anticipated the respiration levels were activated in *SSG1-1* mutant. I analyzed the amount of transcription levels of *COX3,* the mitochondrial electron transport system complex subunit gene (Fig. 6F) (Yong, and Shadel, 2009). The *COX3* which was a mitochondrial gene was not detected by microarray. As expected, the transcript levels of *COX3* in *SSG1-1* mutant were more increased than that of WT cells (Fig. 6F). Furthermore, I analyzed whether Snf1 was activated by administration of SAM or SAH (Fig. 6G). As a result, Snf1 did not activated by administration of SAM but was activated by administration of SAH (Fig. 6G). It was speculated that SAH promoted activation of Snf1 associated with stimulating synthesis of SAM.

Deleting *SAM1* or *SAM2* slightly extended the maximum CLS (Fig. 2C). To test whether *sam1*Δ and *sam2*Δ cells extends CLS by activation of Snf1, I also examined Snf1 activity in these mutants (Fig. 6H). Although, these mutants didn't accumulate SAM compared with WT cells (Fig. 2B), activation levels of Snf1 were increased in both cells (Fig. 6H), suggesting that *sam1*Δ and *sam2*Δ promoted activation of Snf1 in a different mechanism from stimulating SAM synthesis. This mechanism will be revealed by further study of regulation of lifespan involved in SAM metabolism.

2. 4. 3 Severe CR (0.05% glucose) promoted SAM production dependent on SAM synthetase, leading to extended maximum CLS

What was a physiologically relevant stimulus for SAM synthesis? *S. pombe* cells growing in medium containing a low glucose concentration of around 2.2 mM (about 0.04%) accumulate SAM (Pluskal *et al.*, 2011); and Snf1 activity positively correlates with severe CR (0.05% glucose) (Orlova *et al.*, 2008). Thus, I hypothesized that cells faced with severe CR were channeled into SAM synthesis, which would be beneficial for longevity. I therefore checked whether the amount of SAM would be increased in the case of severe CR. Consistent with the previous report on *S. pombe*, *S. cerevisiae* WT cells also showed a significantly increased SAM level upon severe CR (0.05% glucose) (Fig. 7A). This severe CR increased the maximum CLS of WT cells compared with that for the control cells (2% glucose) (Fig. 7C). I further found that the SAH level was also increased upon severe CR (Fig. 7B), which contributed to the accumulation of SAM as observed in administration of SAH. In contrast, the amount of

SAM and SAH in *sam1Δ* cells upon severe CR remained unchanged (Fig. 7D and 7E), and these cells showed a CLS similar to that of the controls (2% glucose) (Fig. 7F). Taken together, these data indicate that stimulation of SAM synthesis in cells under severe CR contributed to the maintenance of cell viability. Because *SSG1-1* mutants and severe CR-treated cells contained SAH, these results further suggested that SAH triggered the stimulation of SAM synthesis, leading to an extended CLS under these physiological conditions.

Although, glucose starvation (0% glucose) caused a significantly increased SAM level in WT cells (Fig. 7A), no beneficial effect of this increase on CLS was observed (Fig. 7C). Furthermore, CR (0.5% glucose) caused the most beneficial effect on longevity in WT and *sam1Δ* cells (Fig. 7C and 7F), although SAM and SAH synthesis was not stimulated (Fig. 7A, 7B, 7D, and 7E). Thus, the contribution of stimulation of SAM synthesis to the longevity appears to be specific to the severe CR condition.

2. 5 DISCUSSION

Chapter II presented evidence that the *SSG1-1* mutant, which stimulated SAM synthesis, consumed Met and ATP (Fig. 5D and 5E) and activated Snf1 (Fig. 5A). It turned on a metabolic switch that resulted in enhanced stress resistance (Fig. 1H) and longevity (Fig. 1D). The accumulation of SAM and SAH occurred during severe CR (0.05% glucose) and were important for the extension of CLS in severe CR (Fig. 7A). The results suggested that Met metabolism affected the lifespan through the stimulation of SAM synthesis.

Deleting *SAM1* or *SAM2* slightly extended the maximum CLS compared with that of WT cells (Fig. 2C), consistent with the observations that the RNA interference knock-down of *sams-1* (SAM synthetase of *C. elegans*) in adults increased the lifespan of *C. elegans* and that *sams-1* loss-of-function mutants displayed an increased lifespan (Hansen *et al.*, 2005; Cabreiro *et al.*, 2013). Sam1/2 was required for Met and ATP to synthesize SAM and *sam1Δ sam2Δ* double-mutant cells displayed SAM auxotrophy (Thomas, and Surdin-Kerjan, 1997). Hence, decreased methylation capacity (*sam1Δ* or *sam2Δ*) might allow a cell to sense Met or ATP restriction. Indeed, presently Snf1 activity was elevated in the *sam1Δ* or *sam2Δ* cells (Fig. 6H).

At this point, it was unknown why CR (0.5% glucose) caused the most

beneficial effect on longevity, although glucose starvation (0% glucose) had a detrimental effect on CLS (Fig. 7C). A previous study showed that CR maintained consistent ATP levels by enhancing mitochondrial metabolism during chronological aging (Choi, and Lee, 2013). Consistent with this finding, *SSG1-1* cells displayed increased ATP levels during the exponential growth phase (Fig. 5E). By contrast, acute glucose starvation might not be able to maintain ATP levels. It was possible that there might be a certain threshold concentration of glucose that maintained mitochondrial function, contributing to the extension of the CLS of yeast.

Recent studies documented that Met metabolism could regulate lifespan in diverse model organisms (Obata, and Miura, 2015, Schosserer, *et al*., 2015). In yeast, MR extended the lifespan by maintaining vacuolar acidification (Sutter, *et al.*, 2013) and decreasing TOR activation (Ruckenstuhl*, et al.,* 2014; Lee*, et al.*, 2014). In *D. melanogaster*, overexpression of Tsc2, which controls cellular growth via the insulin and TOR signaling pathways, inhibited lifespan extension by MR. The present finding that intracellular levels of Met were decreased in *SSG1* cells compared of WT cells (Fig 5D) prompted the expectation that *SSG1-1* cells would have decreased activation levels of TOR. It was reported that vacuolar acidification contributed to the maintenance mitochondrial function during aging (Hughes, and Gottschling 2012). Because the *SSG1-1* mutant activated the expression levels of *COX3* (Fig. 6F), *SSG1-1* cells might also maintain acidification in vacuole to activate the mitochondrial function.

SAM and SAH reportedly regulated the activation of the TOR pathway (Gu *et al.*, 2017; Sutter *et al.*, 2013). In human cells, SAMTOR was identified as a negative regulator of mammalian TOR complex 1 (mTORC1) responding to accumulate levels of intracellular SAM. When intracellular SAM levels increased, SAMTOR was inhibited by binding of SAM and dissociated from mTORC1, which resulted in activated mTORC1 (Gu *et al.*, 2017). In yeast, protein phosphatase 2A, PP2A, could be methylated and activated TORC1 (Sutter *et al.*, 2013). Therefore, SAM or SAH might regulate lifespan via regulation of the TOR pathway.

Presently, a unique effect of SAH that contributed to the activation of Snf1 was evident (Fig. 6G) and led to longevity (Fig. 3A). However, the mechanism of the stimulated SAM synthesis by administration of SAH remains unclear. A recent study (Pendreton, *et al.*, 2017) attempted to explain the mechanism of regulation of intracellular SAM synthesis in human cells responding to environmental nutrition levels. They found that when extracellular Met levels decreased the intron of MAT2ARNA, the

RNA of SAM synthetase in human cells, was spliced and protein synthesis of MAT2A was activated to maintain intracellular SAM levels. The authors suggested that intracellular SAM levels were regulated in response to intracellular Met levels.

SAH inhibits methylation reaction and leads to detrimental effects in the host (Xiao, *et al.*, 2015). However, presently a low dosage of SAH extended the yeast CLS (Fig. 3A). Therefore, it was expected that SAH is a key metabolite in the regulation of lifespan controlling physiological function.

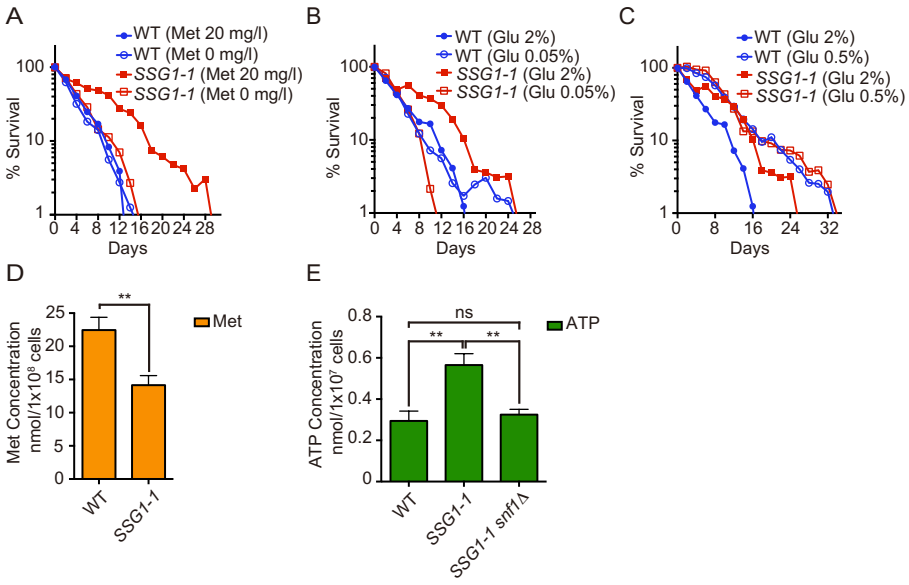

Fig. 5 Stimulating SAM synthesis-mediated longevity was epistatic to CR.[#]

(A–C) *SSG1-1* cells required Met or glucose for longevity. CLS curves were shown. Met (D) and ATP levels (E) of cells were shown. ns, not significant; $^{**}P < 0.01$ (*t* test, two-tailed, parametric unequal variance). # Fig. 5 was cited and modified from Ogawa *et al.*, 2016.

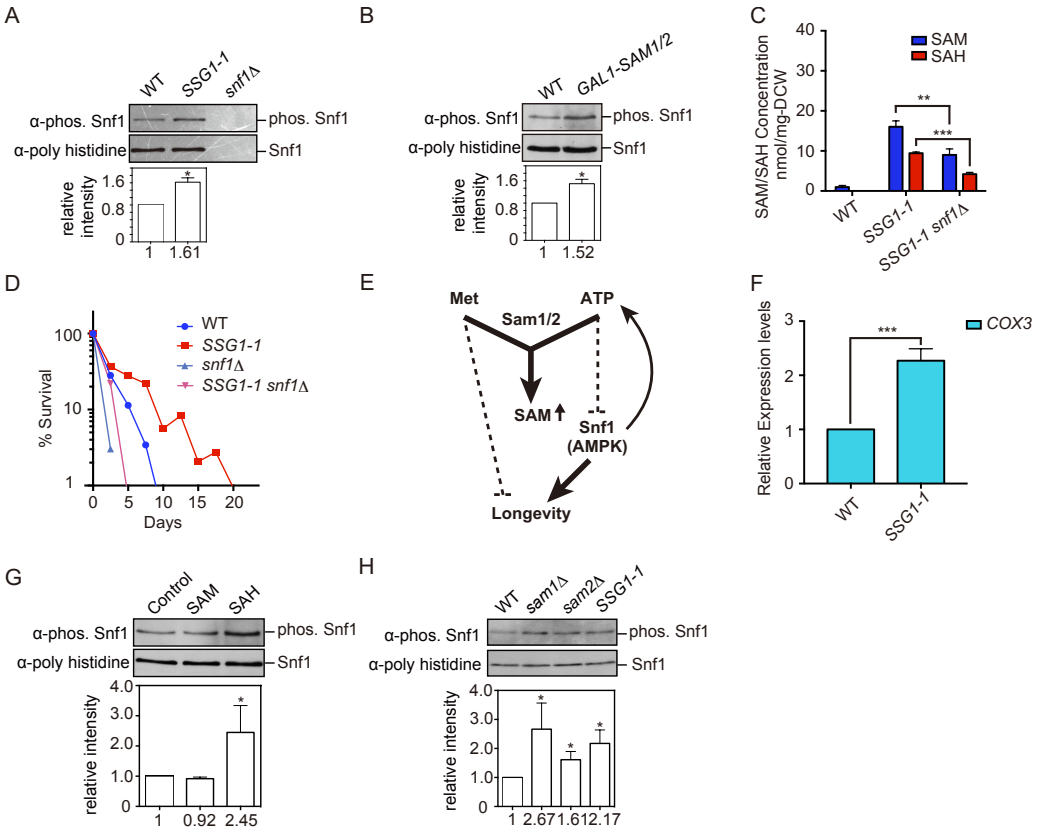

Fig. 6 Stimulating SAM synthesis led to AMPK activation.[#]

(A, B, G, H) Phosphorylation levels of Snf1 residue Thr210 in (A) *SSG1-1* cells, (H) *sam1*Δ and *sam2*Δ cells. Effect of (B) overexpression of *SAM1* and *SAM2* or (G) administration of SAM and SAH on Snf1 phosphorylation levels. Phosphorylation levels were quantified by ImageJ, and relative intensity normalized to total Snf1 is indicated below each band. Mean ± SD (n = 3); **P* < 0.05 (*t* test, two-tailed, parametric unequal variance). (C) The SAM and SAH contents were measured. Mean ± SD (n = 3); ***P* < 0.01; ****P* < 0.001 (*t* test, two-tailed, parametric unequal variance). (D) CLS curve is shown. (E) Model for stimulated SAM synthesis-mediated longevity in yeast. (F) Relative expression level of *COX3* measured by reverse transcription real time PCR.

Fig. 6 was cited and modified from Ogawa *et al.*, 2016.

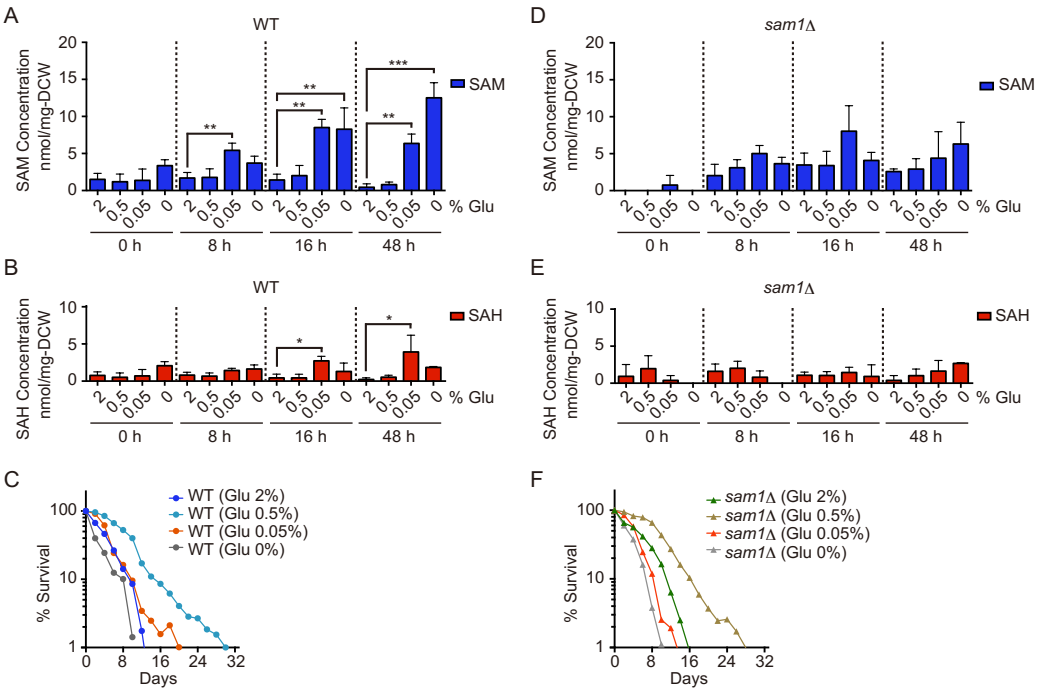

Fig. 7 Severe CR (0.05% glucose) promoted SAM production dependent on SAM synthetase, leading to extended maximum CLS.[#]

Intracellular SAM (A and D) and SAH levels (B and E) or CLS (C and F) under several glucose-limited conditions were shown. Intracellular SAM and SAH levels were quantified. Mean ± SD (n = 3). **P* < 0.05; ***P* < 0.01; ****P* < 0.001 (one-way ANOVA with Tukey's multiple comparisons test; A, B, D, and E). # Fig. 7 was cited and modified from Ogawa *et al.*, 2016.

Table 3 Strains used in Chapter II

Strain	Genotype	Source or Reference
W303-1A	MATa; *trp1, leu2, ade2, ura3, his3, can1-100*	Lab. stock
YMM222	MATa; *sah1-1* [W303-1A]	Mizunuma *et al*., 2004
YRT15	MATa; *SSG1-1* [W303-1A]	Chapter I
YRT3	MATa; *sah1-1 SSG1-1* [W303-1A]	Chapter I
YTK22	MATa; *snf1Δ::kanMX4* [W303-1A]	this study
YTK23	MATa; *SSG1-1 snf1Δ::kanMX4* [W303-1A]	this study
YTO29	MATa; *sam1Δ::kanMX4* [W303-1A]	Chapter I
YTO35	MATa; *sam2Δ::kanMX4* [W303-1A]	Chapter I
YTO78	MATa; *GAL1-SAM1 GAL1-SAM2* [W303-1A]	Chapter I

Table 4 Significant up-regulated genes in the *SSG1-1* strains relative to WT strains

Systematic Name	Standard Name	Ratio (*SSG1-1* vs. WT)	*P* value	Description
YLR301W	*HRI1*	9.58	0.0216	Protein of unknown function
YFR053C	*HXK1*	7.97	0.0522	Hexokinase isoenzyme 1
YLR327C	*TMA10*	5.88	0.0616	Protein of unknown function
YHR092C	*HXT4*	4.07	0.0130	High-affinity glucose transporter
YDR277C	*MTH1*	3.47	0.0012	Negative regulator of the glucose-sensing signal transduction pathway
YLR312C	*ATG39*	3.34	0.0070	Autophagy receptor with a role in degradation of the ER and nucleus
YBR296C	*PHO89*	2.83	0.0603	Plasma membrane Na+/Pi cotransporter
YLL062C	*MHT1*	2.72	0.0283	*S*-methylmethionine-homocysteine methyltransferase
YMR251W	*GTO3*	2.72	0.0068	Omega class glutathione transferase
YMR280C	*CAT8*	2.43	0.0059	Zinc cluster transcriptional activator
YFR023W	*PES4*	2.37	0.0447	Poly (A) binding protein
YKL001C	*MET14*	2.27	0.0177	Adenylylsulfate kinase
YLR092W	*SUL2*	2.25	0.0019	High affinity sulfate permease
YJR010W	*MET3*	2.24	0.0383	ATP sulfurylase
YMR303C	*ADH2*	2.21	0.0237	Glucose-repressible alcohol dehydrogenase II
YBR285W	---	2.18	0.0008	Putative protein of unknown function
YAL067C	*SEO1*	2.15	0.0013	Putative permease
YOR382W	*FIT2*	2.08	0.0025	Mannoprotein that is incorporated into the cell wall
YML054C	*CYB2*	2.06	0.0270	Cytochrome b2 (L-lactate cytochrome-c oxidoreductase)
YDL181W	*INH1*	2.04	0.0041	Protein that inhibits ATP hydrolysis by the F1F0-ATP synthase
YKL217W	*JEN1*	2.03	0.0060	Monocarboxylate/proton symporter of the plasma membrane

Table 5 *P* values for chronological lifespan analysis

Figure	Strain A	Strain B	*P*-value against B
Fig. 5A	WT (Met 20 mg/l)	*SSG1-1* (Met 20 mg/l)	< 0.0001
	WT (Met 20 mg/l)	WT (Met 0 mg/l)	0.0490
	SSG1-1 (Met 20 mg/l)	*SSG1-1* (Met 0 mg/l)	< 0.0001
	WT (Met 0 mg/l)	*SSG1-1* (Met 0 mg/l)	0.0002
Fig. 5B	WT (Glu 2%)	*SSG1-1* (Glu 2%)	< 0.0001
	WT (Glu 2%)	WT (Glu 0.05%)	0.9974
	SSG1-1 (Glu 2%)	*SSG1-1* (Glu 0.05%)	< 0.0001
	WT (Glu 0.05%)	*SSG1-1* (Glu 0.05%)	0.9764
Fig. 5C	WT (Glu 2%)	*SSG1-1* (Glu 2%)	< 0.0001
	WT (Glu 2%)	WT (Glu 0.5%)	< 0.0001
	SSG1-1 (Glu 2%)	*SSG1-1* (Glu 0.5%)	< 0.0001
	WT (Glu 0.5%)	*SSG1-1* (Glu 0.5%)	0.2026
Fig. 6D	WT	*snf1*Δ	< 0.0001
	WT	*SSG1-1 snf1*Δ	0.0671
	SSG1-1	*SSG1-1 snf1*Δ	< 0.0001
Fig. 7C	WT (Glu 2%)	WT (Glu 0.5%)	< 0.0001
	WT (Glu 2%)	WT (Glu 0.05%)	0.0023
	WT (Glu 2%)	WT (Glu 0%)	< 0.0001
	WT (Glu 0.5%)	WT (Glu 0.05%)	< 0.0001
	WT (Glu 0.05%)	WT (Glu 0%)	< 0.0001
Fig. 7F	*sam1*Δ (Glu 2%)	*sam1*Δ (Glu 0.5%)	< 0.0001
	*sam1*Δ (Glu 2%)	*sam1*Δ (Glu 0.05%)	0.4930
	*sam1*Δ (Glu 2%)	*sam1*Δ (Glu 0%)	0.0002
	*sam1*Δ (Glu 0.5%)	*sam1*Δ (Glu 0.05%)	< 0.0001
	*sam1*Δ (Glu 0.05%)	*sam1*Δ (Glu 0%)	0.0289

P values were derived from a two-way ANOVA with time and strain used as independent factors.

CONCLUDING REMARKS

Aging is a universal physiological phenomenon in diverse organisms from prokaryotes to mammals. It is a complex process that is attributable to the accumulation of various molecular, cellular, and organ damages that lead to diseases and death. Despite its complexity, the aging process and many other biological processes are subject to regulation by signaling pathways and transcription factors (Kenyon, 2005; Kenyon, 2010; Fontana *et al.*, 2010).

Dietary and genetic alternations can extend the lifespan of various model organisms. The budding yeast, *S. cerevisiae,* has emerged as a versatile and robust model system of eukaryotic cells. Genetic and molecular analyses are simpler and easier to perform in yeast than in multicellular organisms. Therefore, *S. cerevisiae* is a powerful analytical tool for understanding the molecular mechanisms of highly complex signaling pathways in higher eukaryotes such as humans (Botstein, and Fink, 2011).

Different signaling pathways, transcriptional pathways, and transcription factors coordinate the expression of stress-response genes in yeast. Moreover, yeast cells are a useful model for aging research, and have been instrumental in the identification of new longevity genes and pathway in higher eukaryotes. How much of what we have learned about signaling pathways in yeast are relevant to humans is an important issue. Although some aspects of yeast signaling pathways are specific to this organism, the evidence so far suggests that many of the most important features have been evolutionary conserved in mammals.

The Ras/cAMP-dependent protein kinase (PKA) pathway is a highly conserved pathway of lifespan regulation that was discovered from budding yeasts (Fontana *et al.*, 2010). PKA-mediated signal transduction involves activation by cAMP and regulates many physiological functions including the stress response, triglyceride storage, and cell growth. Loss of function of adenyl cyclase Cyr1 or inactivation of a component of PKA such as Tpk1, Tpk2, and Tpk3 extended the lifespan. PKA mutation in rodents could also increase lifespan (Wei, *et al.,* 2003; Fontana *et al.*, 2010). These results suggested that the lifespan of humans might be regulated by PKA signaling. In recent studies, our laboratory found that PKA phosphorylates and inactivates Whi3, which is the negative regulator of cyclin, *CLN3* (Mizunuma *et al*., 2013a, Mizunuma *et al.*, 2013b). Therefore, Whi3 might also regulate lifespan in yeast.

In recent studies, several metabolites modulated activation levels of some signaling pathways to regulate lifespan. In particular, N-acylethanolamine treatment in

risks-1 mutants, which had a defect in the worm ortholog of S6 kinase of the TOR pathway, suppressed the longevity phenotype (Lucanic, *et al.*, 2011). The α-ketoglutarate decreased TOR pathway activity and increased AMPK activity through the inhibition of ATP synthase in *C. elegans* (Chin, *et al.*, 2014). Decreasing the levels of hydrogen sulfide by activation of TOR pathway could suppress longevity of DR in mice (Hine, *et al.*, 2015). Although these studies suggested that metabolism and aging were intimately linked, how Met metabolites affected lifespan remained unclear.

The present data revealed that stimulating SAM synthesis modulated the activation of AMPK, which resulted in the extension of CLS in yeast. Chapter I revealed that stimulating SAM synthesis extended CLS in the *SSG1-1* mutant. The data presented in Chapter II demonstrated that the *SSG1-1* mutant consumed Met and ATP, which induced the activation of AMPK. Moreover, SAH also activated AMPK and increased CLS by stimulating SAM synthesis.

SAM is related to the regulation of epigenetic gene expression by chromatin methylation (Lopez *et al.*, 2016). This regulation determines diverse physiological functions such as development, differentiation, and aging. Aging and cancer cause abnormalities of DNA methylation in multiple cellular organisms (Lopez *et al.*, 2016). Moreover, epigenetic DNA methylation can be inherited over generations (Lopez *et al.*, 2016). In particular, parental obesity or other metabolic alterations experienced during gestation and lactation led to the transmission of some aspects of metabolic syndrome to the next generation (Lopez *et al.*, 2016). These studies suggested that SAM might regulate aging of descendants by methylation.

In humans, SAH had received much attention as a risk factor for many diseases including vascular and neurodegenerative diseases (Xiao *et al.*, 2015). The present findings of this recently recognized effect of SAH provided new insights into the role played by SAH in human health.

Many of the effects of DR on longevity in model organisms had been linked to reduced protein and amino acid intake (Mair, 2008; Fontana *et al*., 2010; Kaeberlein, 2010). Presently, the stimulation of SAM synthesis *per se* in yeast could produce physiological conditions that mimicked CR. In mammals, the CR benefits included reduced morbidity of a host of diseases, such as cancer and diabetes (Fontana *et al*., 2010). Thus, novel interventions that stimulate SAM synthesis could delay age-related disorders and might even have therapeutic potential in the treatment of major age-related pathologies such as Alzheimer's disease.

REFERENCES

Akao, T., Yashiro, I., Hosoyama, A., Kitagaki, H., Horikawa, H., Watanabe, D., Akada, R., Ando, Y., Harashima, S., Inoue, T. et al. (2011). Whole-genome sequencing of sake yeast Saccharomyces cerevisiae Kyokai no. 7. DNA Res. *18*, 423-434.

Barzilai, N., Huffman, D.M., Muzumdar, R.H., and Bartke, A. (2012). The critical role of metabolic pathways in aging. Diabetes *61*, 1315-1322.

Botstein, D., and Fink, G.R. (2011). Yeast: an experimental organism for 21st century biology. Genetics *189*, 695-704.

Chan, S.Y., and Appling, D.R. (2003). Regulation of S-adenosylmethionine levels in Saccharomyces cerevisiae. J. Biol. Chem. *278*, 43051-43059.

Chin, R.M., Fu, X., Pai, M.Y., Vergnes, L., Hwang, H., Deng, G., Diep, S., Lomenick, B., Meli, V.S., Monsalve, G.C. et al. (2014). The metabolite α-ketoglutarate extends lifespan by inhibiting ATP synthase and TOR. Nature *510*, 397-401.

Choi, J.-S., and Lee, C.-K. (2013). Maintenance of cellular ATP level by caloric restriction correlates chronological survival of budding yeast. Biochem. Biophys. Res. Commun. *439*, 126-131.

Christopher, S.A., Melnyk, S., James, S.J., and Kruger, W.D. (2002). S-adenosylhomocysteine, but not homocysteine, is toxic to yeast lacking cystathionine β-synthase. Mol. Genet. Metab. *75*, 335-343.

Eisenberg, T., Knauer, H., Schauer, A., Büttner, S., Ruckenstuhl, C., Carmona-Gutierrez, D., Ring, J., Schroeder, S., Magnes, C., Antonacci, L. et al. (2009). Induction of autophagy by spermidine promotes longevity. Nat. Cell Biol. *11*, 1305-1314.

Fabrizio, P., Liou, L.L., Moy, V.N., Diaspro, A., SelverstoneValentine, J., Gralla, E.B., and Longo, V.D. (2003). SOD2 functions downstream of Sch9 to extend longevity in yeast. Genetics *163*, 35-46.

Fabrizio, P., and Longo, V.D. (2003). The chronological life span of Saccharomyces cerevisiae. Aging Cell *2*, 73-81.

Fontana, L., Partridge, L., and Longo, V.D. (2010). Extending healthy life span--from yeast to humans. Science *328*, 321-326.

Ghillebert, R., Swinnen, E., Wen, J., Vandesteene, L., Ramon, M., Norga, K., Rolland, F., and Winderickx, J. (2011). The AMPK/SNF1/SnRK1 fuel gauge and energy regulator: structure, function and regulation. FEBS J. *278*, 3978-3990.

Greer, E.L., Maures, T.J., Hauswirth, A.G., Green, E.M., Leeman, D.S., Maro, G.S., Han, S., Banko, M.R., Gozani, O., and Brunet, A. (2010). Members of the H3K4 trimethylation complex regulate lifespan in a germline-dependent manner in C. elegans. Nature *466*, 383-387.

Gu, X., Orozco, J.M., Saxton, R.A., Condon, K.J., Liu, G.Y., Krawczyk, P.A., Scaria, S.M., Harper, J.W., Gygi, S.P., and Sabatini, D.M. (2017). SAMTOR is an S-adenosylmethionine sensor for the mTORC1 pathway. Science *358*, 813-818.

Hansen, M., Hsu, A.-L., Dillin, A., and Kenyon, C. (2005). New genes tied to endocrine, metabolic, and dietary regulation of lifespan from a Caenorhabditis elegans genomic RNAi screen. PLoS Genet. *1*, e17.

Hedbacker, K., and Carlson, M. (2008). SNF1/AMPK pathways in yeast. Front. Biosci. *13*, 2408-2420.

Hine, C., Harputlugil, E., Zhang, Y., Ruckenstuhl, C., Lee, B.C., Brace, L., Longchamp, A., Treviño-Villarreal, J.H., Mejia, P., Ozaki, C.K. et al.(2015). Endogenous hydrogen sulfide production is essential for dietary restriction benefits. Cell *160*, 132-144.

Hughes, A.L., and Gottschling D.E. (2012). An early age increase in vacuolar pH limits mitochondrial function and lifespan in yeast. Nature *492* 261-265.

Ingenbleek, Y., and Kimura, H. (2013). Nutritional essentiality of sulfur in health and disease. Nutr. Rev. *71*, 413–432.

Jacquemin-Faure, I., Thomas, D., Laporte, J., Cibert, C., and Surdin-Kerjan, Y. (1994). The vacuolar compartment is required for sulfur amino acid homeostasis in Saccharomyces cerevisiae. Mol. Gen. Genet. *244*, 519-529.

Johnson, S.C., Rabinovitch, P.S., and Kaeberlein, M. (2013). mTOR is a key modulator of ageing and age-related disease. Nature *493*, 338-345.

Kaeberlein, M., McVey, M., and Guarente, L. (1999). The SIR2/3/4 complex and SIR2 alone promote longevity in Saccharomyces cerevisiae by two different mechanisms. Genes Dev. *13*, 2570–2580

Kanai, M., Kawata, T., Yoshida, Y., Kita, Y., Ogawa, T., Mizunuma, M., Watanabe, D., Shimoi, H., Mizuno, A., Yamada, O. et al. (2017). Sake yeast YHR032W/ERC1 haplotype contributes to high S-adenosylmethionine accumulation in sake yeast strains. J. Biosci. Bioeng. *123*, 8-14.

Kanai, M., Masuda, M., Takaoka, Y., Ikeda, H., Masaki, K., Fujii, T., and Iefuji, H. (2013). Adenosine kinase-deficient mutant of Saccharomyces cerevisiae accumulates S-adenosylmethionine because of an enhanced methionine biosynthesis pathway. Appl. Microbiol. Biotech. *97*, 1183-1190.

Kenyon, C. (2005). The plasticity of aging: insights from long-lived mutants. Cell *120*, 449-460.

Kenyon, C.J. (2010). The genetics of ageing. Nature *467*, 622-622.

Lee, B.C., Kaya, A., Ma, S., Kim, G., Gerashchenko, M.V., Yim, S.H., Hu, Z., Harshman, L.G., and Gladyshev, V.N. (2014). Methionine restriction extends lifespan of Drosophila melanogaster under conditions of low amino-acid status. Nat. Commun. *5*, 3592.

Lee, C., and Longo, V.D. (2011). Fasting vs dietary restriction in cellular protection and cancer treatment: from model organisms to patients. Oncogene *30*, 3305-3316.

Lee, S.-W., Park, B.-S., Choi, E.-S., and Oh, M.-K. (2010). Overexpression of ethionine resistance gene for maximized production of S-adenosylmethionine in Saccharomyces cerevisiae sake kyokai No. 6. Korean J. Chem. Eng. *27*, 587-589.

Lee, Y.-L., and Lee, C.-K. (2008). Transcriptional response according to strength of calorie restriction in Saccharomyces cerevisiae. Mol. Cells *26*, 299-307.

Lin, S.-J., Defossez, P.-A., and Guarente, L. (2000). Requirement of NAD and SIR2 for life-span extension by calorie restriction in Saccharomyces cerevisiae. Science *289*, 2126–2128

Longo, V.D., and Kennedy, B.K. (2006). Sirtuins in aging and age-related disease. Cell *126*, 257-268.

Longtine, M.S., McKenzie, A. 3rd, Demarini, D.J., Shah, N.G., Wach, A., Brachat, A., Philippsen, P., and Pringle, J.R. (1998). Additional modules for versatile and economical PCR-based gene deletion and modification in Saccharomyces cerevisiae. Yeast *14*, 953-961.

López-Otín, C., Blasco, M.A., Partridge, L., Serrano, M., and Kroemer, G. (2013). The hallmarks of aging. Cell *153*, 1194-1217.

López-Otín, C., Galluzzi, L., Freije, J.M.P., Madeo, F., and Kroemer, G. (2016). Metabolic control of longevity. Cell *166*, 802-821.

Lucanic, M., Held, J.M., Vantipalli, M.C., Klang, I.M., Graham, J.B., Gibson, B.W., Lithgow, G.J., and Gill, M.S. (2011). N-acylethanolamine signalling mediates the effect of diet on lifespan in Caenorhabditis elegans. Nature *473*, 226-229.

Mair, W., and Dillin, A. (2008). Aging and survival: the genetics of life span extension by dietary restriction. Annu. Rev. Biochem. *77*, 727-754.

Mayer, F.V., Heath, R., Underwood, E., Sanders, M.J., Carmena, D., McCartney, R.R., Leiper, F.C., Xiao, B., Jing, C., Walker, P.A. et al. (2011). ADP regulates SNF1, the Saccharomyces cerevisiae homolog of AMP-activated protein kinase. Cell Metab. *14*, 707-714.

Miller, R.A., Buehner, G., Chang, Y., Harper, J.M., Sigler, R., and Smith-Wheelock, M. (2005). Methionine-deficient diet extends mouse lifespan, slows immune and lens aging, alters glucose, T4, IGF-I and insulin levels, and increases hepatocyte MIF levels and stress resistance. Aging Cell *4*, 119-125.

Mizunuma, M., Miyamura, K., Hirata, D., Yokoyama, H., and Miyakawa, T. (2004). Involvement of S-adenosylmethionine in G1 cell-cycle regulation in Saccharomyces cerevisiae. Proc. Natl. Acad. Sci. USA *101*, 6086-6091.

Mizunuma, M., Ogawa, T., Koyama, T., Shitamukai, A., Tsubakiyama, R., Komaruyama, T., Yamaguchi, T., Kume, K., and Hirata, D. (2013a). Evidence of antagonistic regulation of restart from G1 delay in response to osmotic stress by the Hog1 and Whi3 in budding yeast. Biosci. Biotech. Biochem. *77*, 2002-2007.

Mizunuma, M., Tsubakiyama, R., Ogawa, T., Shitamukai, A., Kobayashi, Y., Inai, T., Kume, K., and Hirata, D. (2013b). Ras/cAMP-dependent protein kinase (PKA) regulates multiple aspects of cellular events by phosphorylating the Whi3 cell cycle regulator in budding yeast. J. Biol. Chem. *288*, 10558-10566.

Obata, F., and Miura, M. (2015). Enhancing S-adenosyl-methionine catabolism extends Drosophila lifespan. Nat. Commun. *6*, 8332.

Ocampo, A., Liu, J., Schroeder, E.A., Shadel, G.S., and Barrientos, A. (2012). Mitochondrial respiratory thresholds regulate yeast chronological life span and its extension by caloric restriction. Cell Metab. *16*, 55-67.

Ogawa, T., Tsubakiyama, R., Kanai, M., Koyama, T., Fujii, T., Iefuji, H., Soga, T., Kume, K., Miyakawa, T., Hirata, D., and Mizunuma, M. (2016). Stimulating *S*-adenosyl-L-methionine synthesis extends lifespan via activation of AMPK. Proc. Natl. Acad. Sci. USA, *113,* 11913-11918.

Orentreich, N., Matias, J.R., Defelice, A., and Zimmerman, J.A. (1993). Low methionine ingestion by rats extends life span. J. Nutr. *123*, 269-274.

Orlova, M., Barrett, L., and Kuchin, S. (2008). Detection of endogenous Snf1 and its activation state: application to Saccharomyces and Candidaspecies. Yeast *25*, 745-754.

Pendleton, K.E., Chen, B., Liu, K., Hunter, O.V., Xie, Y., Tu, B.P., and Conrad, N.K. (2017). The U6 snRNA m 6 A methyltransferase METTL16 regulates SAM synthetase intron retention. Cell *169*, 824-835.

Pluskal, T., Hayashi, T., Saitoh, S., Fujisawa, A., and Yanagida, M. (2011). Specific biomarkers for stochastic division patterns and starvation-induced quiescence under limited glucose levels in fission yeast. FEBS J. *278*, 1299-1315.

Ruckenstuhl, C., Netzberger, C., Entfellner, I., Carmona-Gutierrez, D., Kickenweiz, T., Stekovic, S., Gleixner, C., Schmid, C., Klug, L., Sorgo, A.G. et al. (2014). Lifespan extension by methionine restriction requires autophagy-dependent vacuolar acidification. PLoS Genet. *10*, e1004347.

Schosserer, M., Minois, N., Angerer, T.B., Amring, M., Dellago, H., Harreither, E., Calle-Perez, A., Pircher, A., Gerstl, M.P., Pfeifenberger, S. et al. (2015). Methylation of ribosomal RNA by NSUN5 is a conserved mechanism modulating organismal lifespan. Nat. Commun. *6*, 6158.

Shimizu, S., Shiozaki, S., Ohshiro, T., and Yamada, H. (1984). Occurrence of S-adenosylhomocysteine hydrolase in prokaryote cells. Characterization of the enzyme from Alcaligenes faecalis and role of the enzyme in the activated methyl cycle. Eur. J. Biochem. *141*, 385-392.

Shiomi, N., Fukuda, H., Fukuda, Y., Murata, K., and Kimura, A. (1991). Nucleotide sequence and characterization of a gene conferring resistance to ethionine in yeast Saccharomyces cerevisiae. J. Ferment. Bioeng. *71*, 211-215.

Sutter, B.M., Wu, X.I., Laxman, S., and Tu, B.P. (2013). Methionine inhibits autophagy and promotes growth by inducing the SAM-responsive methylation of PP2A. Cell *154*, 403-415.

Thomas, D., and Surdinkerjan, Y. (1997). Metabolism of sulfur amino acids in Saccharomyces cerevisiae. Microbiol. Mol. Biol. Rev. *61*, 503-532.

Tsubakiyama, R., Mizunuma, M., Gengyo, A., Yamamoto, J., Kume, K., Miyakawa, T., and Hirata, D., (2011). Implication of Ca^{2+} in the regulation of replicative life span of budding yeast. J. Biol. Chem. *286*, 28681-28687.

Wei, M., Fabrizio, P., Hu, J., Ge, H., Cheng, C., Li, L., and Longo, V.D. (2008). Life span extension by calorie restriction depends on Rim15 and transcription factors downstream of Ras/PKA, Tor, and Sch9. PLoS Genet. *4*, e13.

Wu, Z., Song, L., Liu, S.Q., and Huang, D. (2013). Independent and additive effects of glutamic acid and methionine on yeast longevity. PLoS One *8*, e79319.

Wullschleger, S., Loewith, R., and Hall, M.N. (2006). TOR signaling in growth and metabolism. Cell *124*, 471-484.

Xiao, Y., Su, X., Huang, W., Zhang, J., Peng, C., Huang, H., Wu, X., Xia, M., and Ling, W. (2015). Role of S-adenosylhomocysteine in cardiovascular disease and its potential epigenetic mechanism. Int. J. Biochem. Cell Biol. *67*, 158-166.

ACKNOWLEDGEMENTS

It is my great pleasure to express my hearty thanks to Associate Professor Masaki Mizunuma for his invaluable guidance, criticism, and encouragement.
I am deeply indebted to Visiting Professor Dai Hirata and Assistant Professor Kazunori Kume for their constant invaluable discussion and encouragement.
I am very grateful to Professor Emeritus Tokichi Miyakawa for his helpful suggestion and discussion.
I am grateful to thank for Associate Professor Masaki Mizunuma, Professor Junichi Kato, Professor Akio Kuroda and Professor Seiji Kawamoto for fruitful discussion and carefully reviewing this work.
I am very grateful to Professor Hitoshi Shimoi, Professor Tomoyoshi Soga, Associate Professor Atsuko Isogai, Dr. Tsutomu Fujii, Dr. Haruyuki Iefuji and Dr. Muneyoshi Kanai for technical advice and perform some experiments.
I would like to thank "Mizunuma's Laboratory 2012-2017", Dr. Ryohei Tsubakiyama, Dr. Takayuki Koyano, Yuko Nagao, Tomoyo Hashimoto, Chihiro Hatakeyama, Tetsuya Koyama, Ikko Yamana, Fuminori Ueno, Sayaka Hashimoto, Kumiko Yonekita, Sayuri Kaneko, Masashi Suzuki, Yuto Takeuchi, Kenji Nishikawa, Nao Kondo, Hiromi Mizui, Mayuka Tanetani, Haruka Kondo, Yuika Seo, Kento Sawada, Koji Masumura, Konami Kawata, Yusaku Nakagaki and Saki Ueda for their constant guidance, support and help.
I would also like to thank other members of our laboratory for helpful discussion.
I have been a recipient of Japan Society for the Promotion of Science Fellowship (DC2) from April 2016 to March 2018, which I appreciate very much.

Finally, I would like to thank my parents and family respecting my opinions and supporting me.

RELATED PUBLICATIONS

(1) Stimulating *S*-adenosyl-L-methionine synthesis extends lifespan via activation of AMPK
Takafumi Ogawa, Ryohei Tsubakiyama, Muneyoshi Kanai, Tetsuya Koyama, Tsutomu Fujii, Haruyuki Iefuji, Tomoyoshi Soga, Kazunori Kume, Tokichi Miyakawa, Dai Hirata, and Masaki Mizunuma
Proceedings of the National Academy of Sciences of the United States of America, **113** (42), 11913-11918 (2016).

REFERENCES

(1) Ras/cAMP-dependent protein kinase (PKA) regulates multiple aspects of cellular events by phosphorylating the Whi3 cell cycle regulator in budding yeast
Masaki Mizunuma, Ryohei Tsubakiyama, Takafumi Ogawa, Atsunori Shitamukai, Yoshifumi Kobayashi, Tomomi Inai, Kazunori Kume, and Dai Hirata
The Journal of Biological Chemistry, **288** (15), 10558-10566 (2013).

(2) Evidence of antagonistic regulation of restart from G1 delay in response to osmotic stress by the Hog1 and Whi3 in budding yeast
Masaki Mizunuma, Takafumi Ogawa, Tetsuya Koyama, Atsunori Shitamukai, Ryohei Tsubakiyama, Tadamasa Komaruyama, Toshinaga Yamaguchi, Kazunori Kume, and Dai Hirata
Bioscience, Biotechnology, and Biochemistry, **77** (10), 2002-2007 (2013).

(3) Sake yeast *YHR032W/ERC1* haplotype contributes to high *S*-adenosylmethionine accumulation in sake yeast strains
Muneyoshi Kanai, Tomoko Kawata, Yoshie Yoshida, Yasuko Kita, Takafumi Ogawa, Masaki Mizunuma, Daisuke Watanabe, Hitoshi Shimoi, Akihiro Mizuno, Osamu Yamada, Tsutomu Fujii, and Haruyuki Iefuji
Journal of Bioscience and Bioengineering, **123** (1), 8–14 (2017).

(4) メチオニン代謝が鍵となる酵母の長寿の仕組み
小川貴史、水沼正樹
化学と生物、55 巻、8 号、526-528 頁、2017 年

公表論文

(1) Stimulating *S*-adenosyl-L-methionine synthesis extends lifespan via activation of AMPK
Takafumi Ogawa, Ryohei Tsubakiyama, Muneyoshi Kanai, Tetsuya Koyama, Tsutomu Fujii, Haruyuki Iefuji, Tomoyoshi Soga, Kazunori Kume, Tokichi Miyakawa, Dai Hirata, and Masaki Mizunuma
Proceedings of the National Academy of Sciences of the United States of America, **113** (42), 11913-11918 (2016).

参考論文

(1) Ras/cAMP-dependent protein kinase (PKA) regulates multiple aspects of cellular events by phosphorylating the Whi3 cell cycle regulator in budding yeast
Masaki Mizunuma, Ryohei Tsubakiyama, Takafumi Ogawa, Atsunori Shitamukai, Yoshifumi Kobayashi, Tomomi Inai, Kazunori Kume, and Dai Hirata
The Journal of Biological Chemistry, **288** (15), 10558-10566 (2013).

(2) Evidence of antagonistic regulation of restart from G1 delay in response to osmotic stress by the Hog1 and Whi3 in budding yeast
Masaki Mizunuma, Takafumi Ogawa, Tetsuya Koyama, Atsunori Shitamukai, Ryohei Tsubakiyama, Tadamasa Komaruyama, Toshinaga Yamaguchi, Kazunori Kume, and Dai Hirata
Bioscience, Biotechnology, and Biochemistry, **77** (10), 2002-2007 (2013).

(3) Sake yeast *YHR032W/ERC1* haplotype contributes to high *S*-adenosylmethionine accumulation in sake yeast strains
Muneyoshi Kanai, Tomoko Kawata, Yoshie Yoshida, Yasuko Kita, Takafumi Ogawa, Masaki Mizunuma, Daisuke Watanabe, Hitoshi Shimoi, Akihiro Mizuno, Osamu Yamada, Tsutomu Fujii, and Haruyuki Iefuji
Journal of Bioscience and Bioengineering, **123** (1), 8–14 (2017).

(4) メチオニン代謝が鍵となる酵母の長寿の仕組み
小川貴史、水沼正樹
化学と生物、55 巻、8 号、526-528 頁、2017 年